Title: Expanding the space of protein geometries by computational design of *de novo* fold families

One Sentence Summary:

A computational method to systematically sample loop-helix-loop geometries expands the structure space of designer proteins.

Authors: Xingjie Pan*[1,2], Michael Thompson[1], Yang Zhang[1], Lin Liu[1], James S. Fraser[1,3], Mark J. S. Kelly[4], Tanja Kortemme*[1,2,3,5].

Affiliations:

[1] Department of Bioengineering and Therapeutic Sciences, University of California San Francisco, San Francisco, CA, USA.

[2] UC Berkeley – UCSF Graduate Program in Bioengineering, University of California San Francisco, San Francisco, CA, USA.

[3] Quantitative Biosciences Institute (QBI), University of California San Francisco, San Francisco, CA, USA

[4] Department of Pharmaceutical Chemistry, University of California San Francisco, San Francisco, CA, USA.

[5] Chan Zuckerberg Biohub, San Francisco, CA, USA.

*Correspondence to: xingjiepan@gmail.com; tanjakortemme@gmail.com.

Abstract:

Naturally occurring proteins use a limited set of fold topologies, but vary the precise geometries of structural elements to create distinct shapes optimal for function. Here we present a computational design method termed LUCS that mimics nature's ability to create families of proteins with the same overall fold but precisely tunable geometries. Through near-exhaustive sampling of loop-helix-loop elements, LUCS generates highly diverse geometries encompassing those found in nature but also surpassing known structure space. Biophysical characterization shows that 17 (38%) out of 45 tested LUCS designs were well folded, including 16 with designed non-native geometries. Four experimentally solved structures closely match the designs. LUCS greatly expands the designable structure space and provides a new paradigm for designing proteins with tunable geometries customizable for novel functions.

Main text:

Design of proteins with new and useful architectures and functions requires precise control over molecular geometries[1,2]. In nature, proteins adopt a limited set of protein fold topologies[3-5] that are reused and adapted for different functions. Here we define "topology" as the identity and connectivity of secondary structure elements (**Fig. 1A**). Within a given topology, geometric features including length and orientations of secondary structure elements are often highly variable[3,4]. These considerable geometric differences between proteins with the same topology are necessary as they define the exquisite shape and physicochemical complementarity characteristic of protein functional sites. Creating proteins with new functions *de novo* therefore requires the ability to design proteins not only with different topologies, but also distinct custom-shaped geometries within these topologies optimal for each function (**Fig. 1A**).

Computational design has been successful in mimicking the ability of evolution to generate diverse protein structures spanning helical[6-10], alpha-beta[11-13] and beta-sheet[14,15] fold topologies, including novel folds[16]. However, most design methods do not include explicit mechanisms to vary geometric features within a topology. For instance, successful design methods assemble protein structures from peptide fragments using a definition of the desired fold and topological rules derived from naturally occurring structures[12]. Subsequent iterative cycles of fixed-backbone sequence optimization and fixed-sequence structure minimization[16] refine atomic packing interactions, but do not create substantial changes in geometry. An exception are methods that use parametric equations to sample backbone variation[17] or take advantage of modular protein elements, but these methods are restricted to helical bundles[6,8,10] or repeat protein[18] architectures, respectively.

Here we sought to develop a generalizable computational design approach that mimics the ability of evolution to create considerable geometric variation within a given fold topology (**Fig. 1**). When analyzing geometric variation in existing protein fold families, we found that 84% of naturally occurring fold families contain variations in loop-helix-loop (LHL) elements (**Supplementary Figure S1**). We hence reasoned that a method that systematically samples geometric variation in these units would not only be able to recapitulate a large fraction of geometric diversity in naturally occurring structures but also to create fold families of *de novo* designed proteins with tunable geometries (**Fig. 1B**).

To develop a generalizable method that systematically samples geometries of LHL, we first examined the connecting loop elements in native LHL units. For all LHL loop elements from all CATH superfamilies[3] of non-redundant structures, 72.8% contained ≤ 5 residues (**Supplementary Figure S2A**). We therefore focused on sampling LHL units with loop elements that have 2, 3, 4 and 5 residues. We extracted 313,072 loops connecting to helices from the Rosetta non-redundant fragment database[19] and sorted loops into 12 libraries based on loop length and type of adjacent secondary structure (**Supplementary Table S1**). For each library, only non-redundant loops were kept (**Supplementary Methods**); this procedure yielded between 224 and 5,826 loops per library. The loop libraries had degeneracies (total number of loops divided by the number of non-redundant loops in each library) ranging from 4.4 to 202 (**Supplementary Figure S2B**), indicating that evolution frequently used similar loop structures in different proteins. We therefore reasoned that the identified loop element libraries could also be used to computationally sample novel protein structures that have not been explored by nature.

We developed a protocol called loop-helix-loop unit combinatorial sampling (LUCS, **Fig. 1C**, **Supplementary Figure S3**). LUCS starts with an input protein fold, which can be naturally occurring or as in our case *de novo* designed, and a definition of gaps to insert LHL units. The first step systematically samples all loop element pairs in our libraries (**Supplementary Table S1**). For each gap, all pairs of loops from the libraries are inserted and any loops that clash with the input structure are removed. The second step tests all remaining pairs of loops for supporting LHL units by growing helices from each loop. If helices grown from the two ends meet in the middle, excess residues are removed in the third step and the gap closed by energy minimization with a chain-break penalty and hydrogen bond restraints. Closed LHL units with distorted hydrogen bonds geometries, steric clashes or suboptimal interactions between designed backbones and the environment are discarded (**Supplementary Methods**). In a fourth step, combinations of LHL units at different positions can be screened to yield final structures that have multiple compatible LHL units with systematically sampled lengths and orientations.

To validate the ability of LUCS to generate distinct geometries within given fold topologies, we applied the method to three design problems (**Fig. 1D**). In the first two design problems, we varied one (RO1) or two (RO2) LHL units of a *de novo* designed protein[12] (PDB:2LV8) with a Rossmann fold topology. In the third problem, we varied two LHL units of a *de novo* designed protein[20] (PDB:5TPJ) with an NTF2 fold topology (NT). In principle, LUCS can sample topologies with arbitrary number of LHL units. For the systems we tested, systematic sampling of the geometries of each LHL unit generated approximately 10^4 LHL elements for each gap. To limit the required computing power, we screened 10^6 random combinations of LHL units and generated between 10^4-10^5 final backbone structures for each design problem (**Supplementary Table S2**). We then applied the Rosetta FastDesign protocol (**Supplementary Methods**) to

optimize sequences for all residue positions within 10 Å from the new LHL elements. The number of designed residues for each backbone was between 33 and 87. We note that Rosetta FastDesign also introduces structural changes outside the reshaped LHL elements of the designed fold through gradient-based torsion minimization, although these changes are small (backbone heavy atom root-mean-square deviation (RMSD) < 1 Å). Following sequence design, we filtered the design models computationally using a set of quality criteria that included a minimal number of buried unsatisfied hydrogen bond donors/acceptors, tight atomic packing interactions in the protein core, and compatibility between sequences and local structures (**Supplementary Methods**).

For each of the three design problems, we selected 50 low Rosetta energy[21] designs from models that passed the quality filters and had diverse conformations for further computational characterization. The Rosetta design simulations optimized low-energy sequences given a desired structure. To determine the converse, whether the desired structure is also a low energy conformation given the sequence, we conducted *ab initio* protein structure prediction simulations in Rosetta[22]. For the Rossman fold designs, we required the lowest-energy predicted structure to be within 1 Å Cα RMSD of the design model. For the NTF2 fold designs, we used a less strict criterion requiring a number of low-energy models to be close to the design model, to account for the more difficult problem of sampling native-like structures for proteins larger than 100 amino acids. 10, 25 and 10 designs that passed these tests were chosen for experimental characterization for each of the three design problems, respectively (**Fig. 1D**, **Data S1, S2**). The designed proteins were recombinantly expressed in *E. coli* and purified using His-tag affinity and size exclusion chromatography. For monomeric designs, we measured near-UV circular dichroism (CD) spectra, thermal melts monitored by CD, one dimensional 1H

nuclear magnetic resonance (NMR) spectra and 2-dimensional ^{15}N HSQC NMR spectra to assess formation of stable secondary and tertiary structure. 5/10, 8/25 and 4/10 designs were found to be well folded for each of the three design problems, respectively (**Fig. 1D**, **Supplementary Figure S4**, **Supplementary Table S3**).

To assess whether the designed structures adopted their intended geometries, we solved structures for three designs (RO2-1, RO2-20, and RO2-25) that sampled two LHL units in the Rossmann fold topology using nuclear magnetic resonance spectroscopy (NMR), and one structure for the NTF2 fold topology designs (NT-9) by X-ray crystallography (**Supplementary Methods**, **Supplementary Figure S5**, **Supplementary Tables S4-5**). The experimentally solved Rossmann fold structures closely matched the designed models (**Fig. 2 A-C**), with backbone heavy atom RMSDs between models and solved structures within 1.3 Å, and core hydrophobic side chains in good agreements with the designed models (**Supplementary Figure S6**). Among the loops of the designed LHL units, 5 loops were well converged (pairwise backbone RMSD within the ensemble of NMR models within 1 Å). The backbone heavy atom RMSDs between the converged loops of lowest energy NMR models and designs were within 1.6 Å (**Supplementary Figure S7**). In the crystallographic electron density map obtained at 1.5 Å resolution for the NTF2 fold design (NT-9), strong signal was clearly identifiable inside a surface pocket (**Fig. 2D**), which was interpreted as a bound phospholipid (1,2-diacyl-sn-glycero-3-phosphoethanolamine, see **Supplementary Methods**). The two N- and C-terminal helices (residues 1-20 and 113-128), which had not been reshaped by LUCS, were pushed apart to accommodate the ligand, leading to an overall backbone heavy atom RMSD between design and model of 2.7 Å. However, when excluding the N- and C-termini helices and aligning the remainder of the design, the backbone heavy atom RMSD between the model and

the solved structure was 1.4 Å (**Fig. 2E**). Moreover, the designed side chain packing interactions between the reshaped helices were in excellent agreement with the design (**Fig. 2F**). Taken together, our structural analysis confirmed the designed geometry in the reshaped regions for all 4 designs. The presence of a ligand in the NT-9 design is consistent with the known ability of the NTF2 fold to bind to diverse hydrophobic small molecules, and highlights the exciting possibility to introduce new functions such as ligand binding by reshaping protein geometries.

We next analyzed the magnitude of the geometric differences between our designs. We first compared the backbone heavy atom RMSDs between the reshaped helices of all well folded designs (**Fig. 1D**) after aligning the non-reshaped regions using both the design models and experimentally solved structures (**Fig. 3A, Supplementary Figure S8**). For the designs with one LHL unit reshaped, 18 out of 20 off-diagonal differences are more than 3Å (**Fig. 3A, left**). For the designs with two LHL units reshaped, 55 out of 68 off-diagonal differences are more than 4Å (**Fig. 3A, middle and right**). This scale of variation exceeds the backbone changes generated by existing flexible backbone design methods[23,24] that are typically smaller than 2Å RMSD. For each well-folded design, we also identified the closest existing structures in the protein data bank (PDB) using TM-align[25]. Remarkably, 15 out of the 17 designed LHL units were significantly different (RMSD > 3Å for one LHL reshaped designs and RMSD > 4 Å for two LHL reshaped designs) from their closest match in the PDB (**Fig. 3A, Supplementary Figure S9**), indicating that the design protocol not only generates stable structures with considerable conformational divergence, but also geometries not observed in known structures.

We further analyzed the distribution of sampled geometries and their coverage of designable backbone structure space, where a structure is defined as designable if at least one sequence folds into that structure. As a computational approximation, we defined the models that passed the quality filters after the first iteration of sequence design (**Supplementary Methods**) as designable because they had good core packing, hydrogen bond satisfaction and local sequence structure compatibility with the designed sequence. We projected the center and directions of the helices onto the underlying beta sheets (**Fig. 3B**). The sampled helices from designable models at each position encompassed the distributions derived from native protein structures in the PDB (**Fig. 3B, right panels**). For the NTF2 fold, the distributions sampled in the designs were slightly shifted to the upper left when compared to the distributions in known structures (**Supplementary Figure S8**). This difference could be a result of the presence of a C-terminal helix in our designs occupying the region shown in the right of the space projection, whereas C terminal helices were often missing in the ensemble of known structures. Overall, since the number of known protein structures for a given topology is limited, the structure space covered by the known structures is much sparser than the space covered by the sampled structures. We quantified the size of structure space by dividing the 6-dimensional space of helix centers and orientations into bins (**Supplementary Methods**). For the geometries sampled in this work, the known structures covered between 12 and 26 bins, while LUCS generated structures covered between 63 and 221 bins (**Fig 3C**). The 17 well folded designs (**Fig. 1D**) sampled between 3 and 7 bins for each helix, respectively, and the majority (18/22) of these bins were not covered by known structures (**Fig 3D**). All but one of the well folded designs had at least one helix in a novel bin. Five well folded designs had both helices in novel bins (**Fig 3E**). Taken together, these results show that LUCS generates highly diverse geometries encompassing those found in nature but also exceeding known structure space.

We next sought to understand in more detail how the unique backbone geometries of the designed proteins were defined by the precise details of their non-covalent intramolecular interactions. The three experimentally solved Rossmann fold topology structures had distinct sequence patterns (**Fig. 4A**) resulting in distinct packing arrangements (**Fig. 4B, C**) in their hydrophobic cores. The beta sheets favored beta branched residues as expected, but the side chain sizes varied across different designs and resulted in differential hydrophobic packing. In particular, we observed previously described knob-socket type packing motifs[26] (**Fig. 4C, Supplementary Figure S10**) where nonpolar side chains fit into pockets formed by three residues on helices. These arrangements result in matched geometries between the side chains from sheets and helices that likely contribute to specifying the three-dimensional arrangement of the helices. We also applied tertiary motif analysis using MASTER[27]. For all well-folded designs, we were able to match tertiary motifs to both the designed loops and interacting secondary structure elements (**Supplementary Figure S11**). Moreover, we identified side chains mediating helix-helix, helix-sheet and helix-loop interactions that are similar in our designs and the corresponding matched tertiary motifs (**Fig. 4D**). Despite the close match between the local structures in the design and the tertiary motifs, the source proteins of the motifs had overall structures very different from the designs (**Supplementary Figure S11**). Since no tertiary motif information was used in backbone generation or sidechain design, we conclude that our design protocol, which is guided solely by the LUCS sampling protocol and the Rosetta energy function[21], recapitulated tertiary structure motifs that were used recurrently by nature.

Despite the more than 150,000 structures in the PDB, it is unknown how much backbone structure space is designable, and how much designable space is already covered by known

structures. One way to probe the answers to these questions is by designing novel proteins that systematically explore the backbone space beyond known structures. Here we show that a large number of novel protein geometries can be sampled computationally. The experimentally validated, well-folded designs have geometries distinct from known structures. These results indicate that a large part of designable protein structure remains unexplored.

Previous key achievements in *de novo* design[11-15,20] focused on designing one or a few structures for diverse non-helical-bundle topologies by deriving design rules for specific topologies to identify the most favorable geometries. Proteins designed by this topology-centric strategy have pre-defined secondary structure sizes and loop torsions that are ideal to their topologies. In contrast, natural and LUCS generated structure families adopt non-ideal geometric features such as diverse helix positions, orientations, lengths and conformations of connector elements.

Exploring these non-ideal regions presents extra challenges[28]. The topology-centric strategy typically finds deep energy minima and thereby succeeds in overcoming errors in energy functions. Sampling non-ideal geometric features can result in a smaller energy gap between the desired folded state and alternative states. Nevertheless, we show here that LUCS achieves a remarkably accurate atom-level control over diverse geometries. This success can at least partially be explained by the ability of LUCS to recover stable three-dimensional packing arrangements that are recurrent in nature (**Fig. 4D**, **Supplementary Figure S11**), but without using this information as input. Moreover, LUCS does not require prior definition of structural variation based on design rules identified in native structures[20,29] to generate diverse geometries that sample both known and new structural space. New protocols could exploit this ability to

flexibly tune protein geometries during design simulations while simultaneously building new functional sites. The generalizable strategy underlying LUCS (**Fig. 1C**) could also be used for developing methods that sample other types of protein backbone geometries such as beta sheets.

We envision many applications for LUCS to precisely tune protein geometries for new protein functions that require atom-level control. By sampling LHL units, geometries of protein functional sites can be reshaped for ligand binding or protein-protein recognition. The systematic sampling of protein geometries should also enable designing dynamic proteins[30] that can switch between multiple distinct *de novo* designed conformations. Methods such as LUCS bring control over designable protein geometry space for arbitrary functions within reach.

References and Notes:

1. Baker, D. An exciting but challenging road ahead for computational enzyme design. *Protein Sci* **19**, 1817-9 (2010).
2. Kundert, K. & Kortemme, T. Computational design of structured loops for new protein functions. *Biol Chem* **400**, 275-288 (2019).
3. Dawson, N.L., Lewis, T.E., Das, S., Lees, J.G., Lee, D., Ashford, P., Orengo, C.A. & Sillitoe, I. CATH: an expanded resource to predict protein function through structure and sequence. *Nucleic Acids Res* **45**, D289-D295 (2017).
4. Fox, N.K., Brenner, S.E. & Chandonia, J.M. SCOPe: Structural Classification of Proteins--extended, integrating SCOP and ASTRAL data and classification of new structures. *Nucleic Acids Res* **42**, D304-9 (2014).
5. Hou, J., Jun, S.R., Zhang, C. & Kim, S.H. Global mapping of the protein structure space and application in structure-based inference of protein function. *Proc Natl Acad Sci U S A* **102**, 3651-6 (2005).
6. Huang, P.S., Oberdorfer, G., Xu, C., Pei, X.Y., Nannenga, B.L., Rogers, J.M., DiMaio, F., Gonen, T., Luisi, B. & Baker, D. High thermodynamic stability of parametrically designed helical bundles. *Science* **346**, 481-485 (2014).
7. Jacobs, T.M., Williams, B., Williams, T., Xu, X., Eletsky, A., Federizon, J.F., Szyperski, T. & Kuhlman, B. Design of structurally distinct proteins using strategies inspired by evolution. *Science* **352**, 687-90 (2016).
8. Thomson, A.R., Wood, C.W., Burton, A.J., Bartlett, G.J., Sessions, R.B., Brady, R.L. & Woolfson, D.N. Computational design of water-soluble alpha-helical barrels. *Science* **346**, 485-8 (2014).
9. Hill, R.B., Raleigh, D.P., Lombardi, A. & DeGrado, W.F. De novo design of helical bundles as models for understanding protein folding and function. *Acc Chem Res* **33**, 745-54 (2000).
10. Harbury, P.B., Plecs, J.J., Tidor, B., Alber, T. & Kim, P.S. High-resolution protein design with backbone freedom. *Science* **282**, 1462-7 (1998).
11. Rocklin, G.J., Chidyausiku, T.M., Goreshnik, I., Ford, A., Houliston, S., Lemak, A., Carter, L., Ravichandran, R., Mulligan, V.K., Chevalier, A., Arrowsmith, C.H. & Baker, D. Global analysis of protein folding using massively parallel design, synthesis, and testing. *Science* **357**, 168-175 (2017).
12. Koga, N., Tatsumi-Koga, R., Liu, G., Xiao, R., Acton, T.B., Montelione, G.T. & Baker, D. Principles for designing ideal protein structures. *Nature* **491**, 222-7 (2012).
13. Huang, P.S., Feldmeier, K., Parmeggiani, F., Velasco, D.A.F., Hocker, B. & Baker, D. De novo design of a four-fold symmetric TIM-barrel protein with atomic-level accuracy. *Nat Chem Biol* **12**, 29-34 (2016).
14. Dou, J., Vorobieva, A.A., Sheffler, W., Doyle, L.A., Park, H., Bick, M.J., Mao, B., Foight, G.W., Lee, M.Y., Gagnon, L.A., Carter, L., Sankaran, B., Ovchinnikov, S., Marcos, E., Huang, P.S., Vaughan, J.C., Stoddard, B.L. & Baker, D. De novo design of a fluorescence-activating beta-barrel. *Nature* **561**, 485-491 (2018).
15. Marcos, E., Chidyausiku, T.M., McShan, A.C., Evangelidis, T., Nerli, S., Carter, L., Nivon, L.G., Davis, A., Oberdorfer, G., Tripsianes, K., Sgourakis, N.G. & Baker, D. De novo design of a non-local beta-sheet protein with high stability and accuracy. *Nat Struct Mol Biol* **25**, 1028-1034 (2018).

16. Kuhlman, B., Dantas, G., Ireton, G.C., Varani, G., Stoddard, B.L. & Baker, D. Design of a novel globular protein fold with atomic-level accuracy. *Science* **302**, 1364-8 (2003).
17. Crick, F. The packing of [alpha]-helices: simple coiled-coils. *Acta Crystallographica* **6**, 689-697 (1953).
18. Brunette, T.J., Parmeggiani, F., Huang, P.S., Bhabha, G., Ekiert, D.C., Tsutakawa, S.E., Hura, G.L., Tainer, J.A. & Baker, D. Exploring the repeat protein universe through computational protein design. *Nature* **528**, 580-4 (2015).
19. Gront, D., Kulp, D.W., Vernon, R.M., Strauss, C.E. & Baker, D. Generalized fragment picking in Rosetta: design, protocols and applications. *PLoS One* **6**, e23294 (2011).
20. Marcos, E., Basanta, B., Chidyausiku, T.M., Tang, Y., Oberdorfer, G., Liu, G., Swapna, G.V., Guan, R., Silva, D.A., Dou, J., Pereira, J.H., Xiao, R., Sankaran, B., Zwart, P.H., Montelione, G.T. & Baker, D. Principles for designing proteins with cavities formed by curved beta sheets. *Science* **355**, 201-206 (2017).
21. Park, H., Bradley, P., Greisen, P., Jr., Liu, Y., Mulligan, V.K., Kim, D.E., Baker, D. & DiMaio, F. Simultaneous Optimization of Biomolecular Energy Functions on Features from Small Molecules and Macromolecules. *J Chem Theory Comput* **12**, 6201-6212 (2016).
22. Bradley, P., Misura, K.M. & Baker, D. Toward high-resolution de novo structure prediction for small proteins. *Science* **309**, 1868-71 (2005).
23. Davey, J.A. & Chica, R.A. Multistate Computational Protein Design with Backbone Ensembles. *Methods Mol Biol* **1529**, 161-179 (2017).
24. Ollikainen, N., Smith, C.A., Fraser, J.S. & Kortemme, T. Flexible backbone sampling methods to model and design protein alternative conformations. *Methods Enzymol* **523**, 61-85 (2013).
25. Zhang, Y. & Skolnick, J. TM-align: a protein structure alignment algorithm based on the TM-score. *Nucleic Acids Res* **33**, 2302-9 (2005).
26. Joo, H., Chavan, A.G., Phan, J., Day, R. & Tsai, J. An amino acid packing code for alpha-helical structure and protein design. *J Mol Biol* **419**, 234-54 (2012).
27. Zhou, J. & Grigoryan, G. Rapid search for tertiary fragments reveals protein sequence-structure relationships. *Protein Sci* **24**, 508-24 (2015).
28. Baker, D. What has de novo protein design taught us about protein folding and biophysics? *Protein Sci* **28**, 678-683 (2019).
29. Lin, Y.R., Koga, N., Tatsumi-Koga, R., Liu, G., Clouser, A.F., Montelione, G.T. & Baker, D. Control over overall shape and size in de novo designed proteins. *Proc Natl Acad Sci U S A* **112**, E5478-85 (2015).
30. Davey, J.A., Damry, A.M., Goto, N.K. & Chica, R.A. Rational design of proteins that exchange on functional timescales. *Nat Chem Biol* **13**, 1280-1285 (2017).

Acknowledgments:

We would like to thank Muziyue Wu, Nicholas Hoppe, and members of the Kortemme lab for discussion. **Funding:** This work was supported by a grant from the National Institutes of Health (NIH) (R01-GM110089) to TK and by the UCSF Program for Breakthrough Biomedical Research, funded in part by the Sandler Foundation. We additionally acknowledge the following fellowships: UCSF Discovery Fellowship (XP) and NIH F32 Postdoctoral Fellowship (MT). TK is a Chan Zuckerberg Biohub Investigator. **Author contributions:** XP conceived the idea for the project. XP and TK conceived the computational and experimental approach. XP developed and performed the computational design. XP and YZ performed the majority of the experimental characterization. XP and MJSK determined the NMR structures. XP, MT, LL and JSF determined the crystal structure. JSF, MJSK and TK provided guidance, mentorship and resources. XP and TK wrote the manuscript with contributions from the other authors. **Competing interests:** The authors declare no competing interests. **Data and materials availability:** Coordinates and structure files have been deposited to the Protein Data Bank (PDB) with accession codes 6VG7, 6VGA, 6VGB and 6W90. All other relevant data are available in the main text or the supplementary materials. Rosetta source code is available from rosettacommons.org. Upon publication, constructs will be made available via Addgene.

Supplementary Materials:

Materials and Methods
Fig S1 – S12
Table S1 – S5
Data S1 – S2

Figure Legends:

Figure 1. LUCS sampling strategy to create *de novo* designed protein fold families with tunable geometries. A. In nature, protein fold topologies (left) are diversified to create families of proteins with distinct geometries (right) optimized for function. Alpha-helices are shown as cylinders and beta-strands as arrows. The box shows schematic representations of common types of geometric variation. **B.** The LUCS computational design protocol seeks to mimic the ability of evolution to diversity protein geometries to generate *de novo* designed fold families. **C.** Schematic of the LUCS protocol for sampling LHL geometries. The reshaped LHL units are colored in red and blue. Typical numbers of models generated at major stages of the protocol are indicated. **D.** Designed fold families. Schematic shows fold topologies and design problems (Rossman fold with 1 or 2 reshaped LHL units, and NTF2 fold with 2 reshaped LHL units). Also shown are numbers for geometries generated by LUCS, designed models that passed quality filters, and experimentally characterized designs for three design problems. % folded indicates the fraction of experimentally tested designs that adopted folded structures.

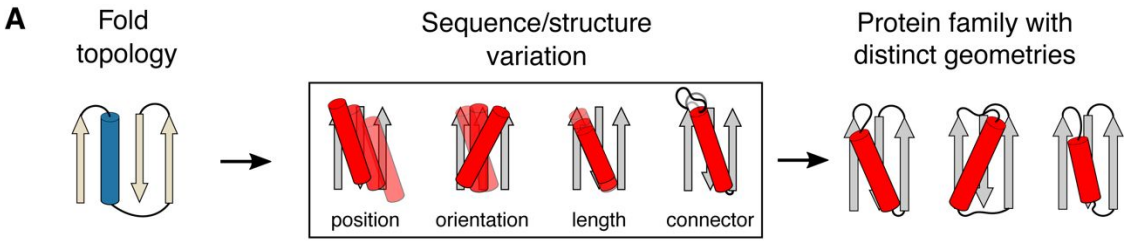

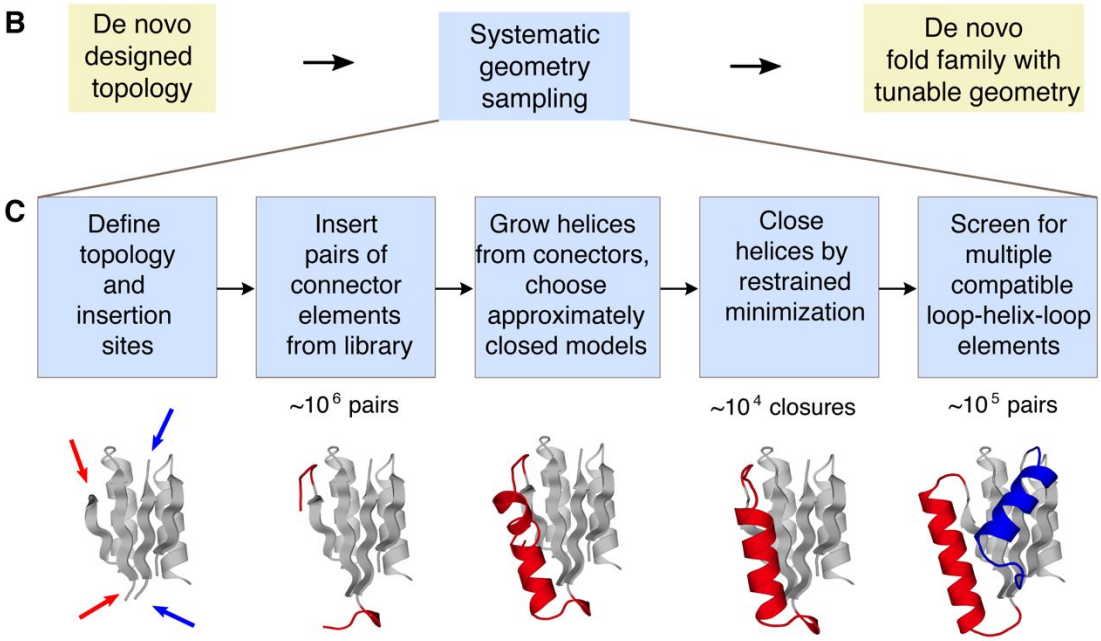

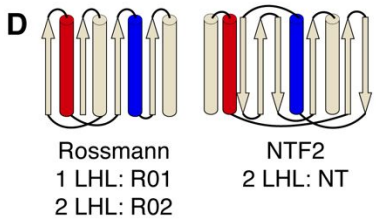

Design Problem	Generated Geometries	Designable Geometries	Designs Selected	Expressed / Purified	Folded (%)
RO1	13,421	1,163	10	6 / 5	5 (50%)
RO2	290,836	9,934	25	14 / 8	8 (32%)
NT	136,683	5,715	10	4 / 4	4 (40%)

Figure 2. Close agreement between models and experimentally determined structures of designed proteins. A-C, designs for the Rossmann fold topology and **D-F,** designs for the NTF2 fold topology. Experimentally determined structures are shown in yellow and design models in grey with the reshaped LHL elements highlighted in red and blue. **A-C.** Comparison between computational models and NMR structures for designs RO2_1(**A**), RO2_20(**B**) and RO2_25(**C**). Also shown are the backbone heavy atom RMSDs calculated using the lowest energy structure from the NMR ensemble. **D**. The binding pocket of a phosphatidylethanolamine ligand. The 2Fo − Fc electron density map (cyan) for the ligand molecule is shown at 1.0 σ level. **E.** Comparison between computational model and X-ray crystal structure for the design NT_9. The phosphatidylethanolamine ligand is shown in spacefill representation (carbon atoms in yellow, oxygen atoms in red, phosphorus atoms in orange, and nitrogen atoms in blue). Also shown are the backbone heavy atom RMSDs calculated including or excluding the terminal helices, respectively. **F.** Alignment between the designed helices in the computational model and the experimentally solved structure. The hydrophobic residues at the packing interface are shown in stick representation. The RMSD shown includes the helix backbone heavy atoms and side chain heavy atoms displayed as sticks.

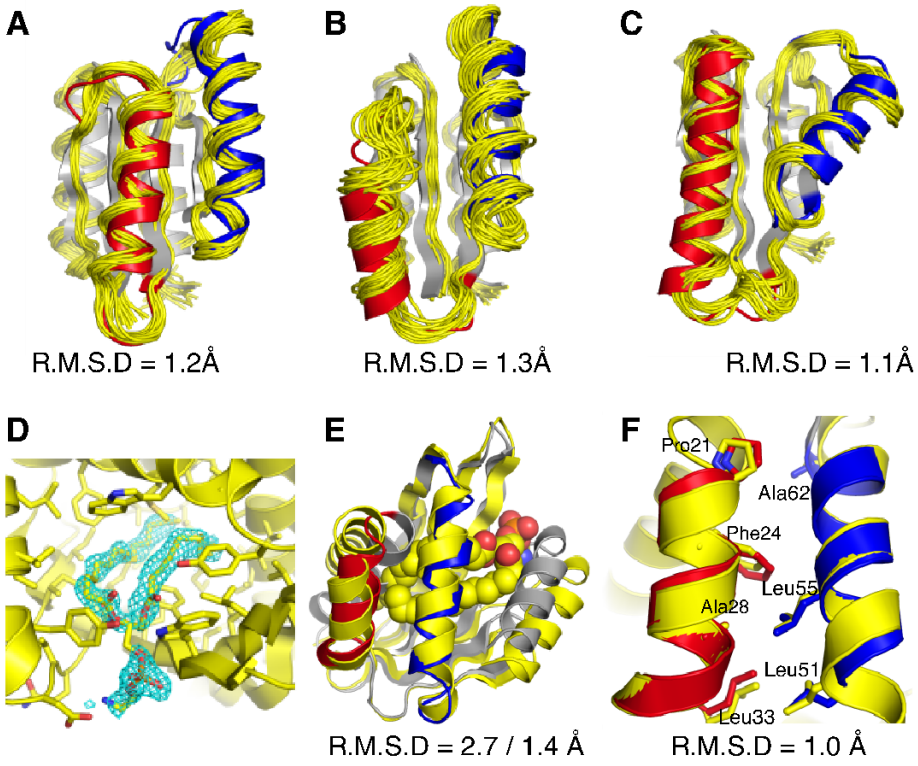

Figure 3. Geometry space sampled by de *novo* designed fold families. In **A** and **B**, the columns show the 3 design problems: Left, Rossman fold with one designed LHL unit (RO1); middle, Rossmann fold with two designed LHL units (RO2); right: NTF2 fold with two designed LHL units (NT). **A.** Heatmaps showing backbone RMSDs between the reshaped LHL-regions of well-folded designs, comparing design models (x axis) with experimentally determined structures (_exp) or lowest-scoring models from Rosetta structure prediction (y axis). Green boxes show RMSDs calculated using experimentally solved structures. Red boxes (right columns) show the RMSDs between designs and the closest known structures found by TM-align. **B.** Projection of centers and directions of designed helices onto the underlying beta sheets. For the RO2 (middle) and NT (right) columns, left and right panels show distributions for designs and known structures, respectively. Sampled designable models (Fig. 1D) are represented by small arrows with reshaped helices colored in red and blue. The experimentally confirmed folded designs (Fig. 1D) are represented as bold arrows with yellow boundaries and the experimentally solved structures are represented as bold arrows with green boundaries. Helices are shown on 4 z-level planes based on their distances from the beta-sheet projection plane. For z-levels that have more than 1000 sampled structures, only 1000 randomly selected helices are shown. Projections for known Rossmann fold (middle) and NTF2 fold (right) protein structures are shown with the two helices corresponding to the designed regions colored in orange and cyan. The Rossmann fold structures are from the CATH superfamily 3.40.50.1980 and the NTF2 fold structures are from the CATH superfamily 3.10.450.50. **C.** Number of structure bins occupied by known structures (orange, cyan) and sampled by designable models generated by LUCS (red, blue). **D.** Structure bins occupied by well folded designs. **E.** Classification of the well folded structures by the number of novel structure bins they occupy.

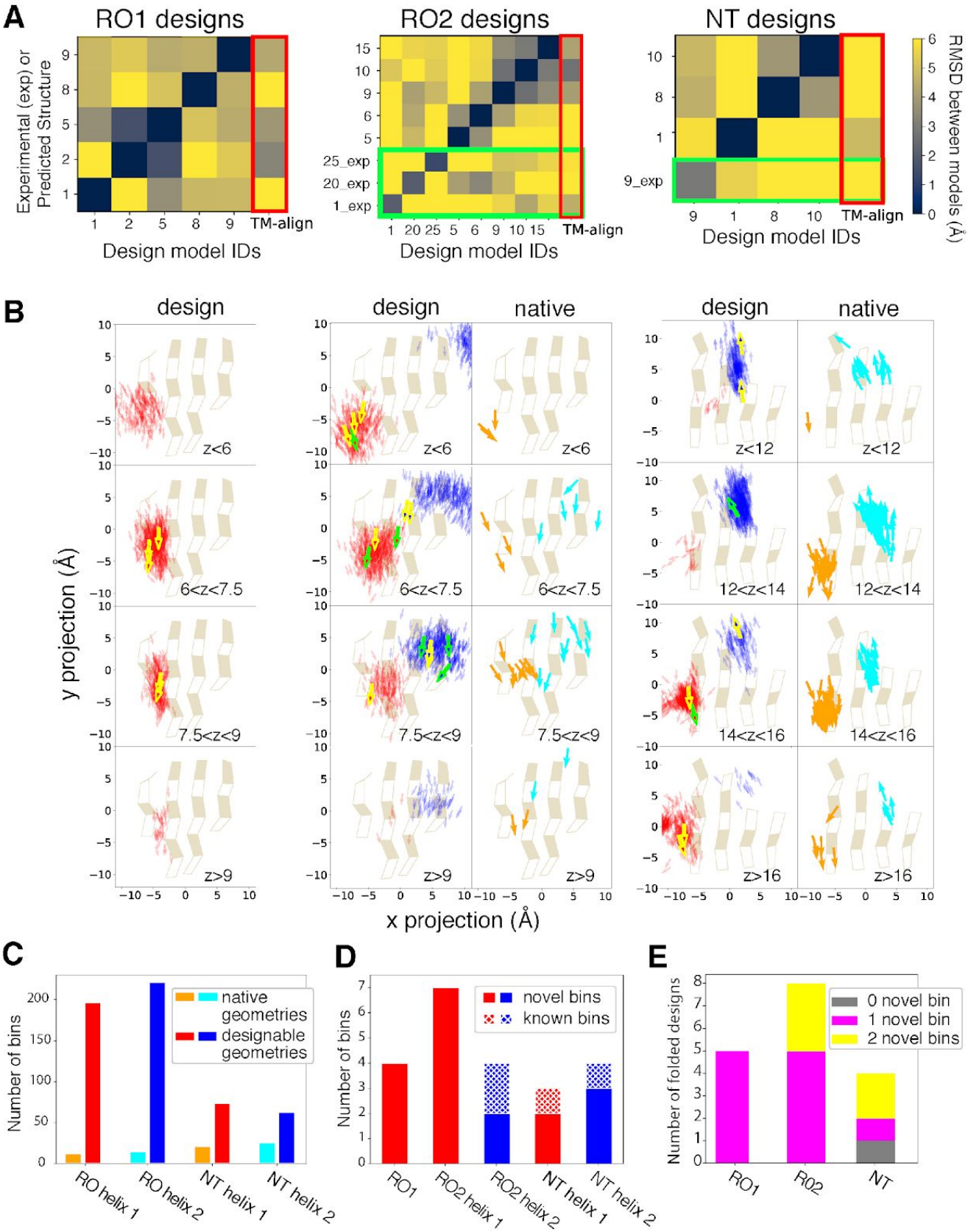

Figure 4. Structural features encoding distinct protein geometries. A. Sequence patterns of the hydrophobic cores in three designed models for the Rossman fold, aligned by corresponding secondary structure elements (top). Hydrophobic residues are shown as letters in rainbow colors ordered by position in the primary protein sequence and scaled by side chain size. Grey underlines indicate positions of surface exposed polar residues. The residues in the boxes are the knob residues shown in (**C**). **B.** Atomic packing of hydrophobic cores in the three experimentally determined structures for the Rossman fold (**Fig. 2**). The hydrophobic side chains in the designed cores are shown as spheres. **C.** Knob-socket packing motifs found in the designs. Three residues on a helix (grey sticks and surfaces) form a socket accommodating a knob residue shown as colored spheres. **D.** Examples of tertiary motifs matching the designed LHL structures. The designed structures are shown in grey and the matched motifs are shown in magenta. Sidechains of the best matched tertiary motifs and design models are shown as sticks.

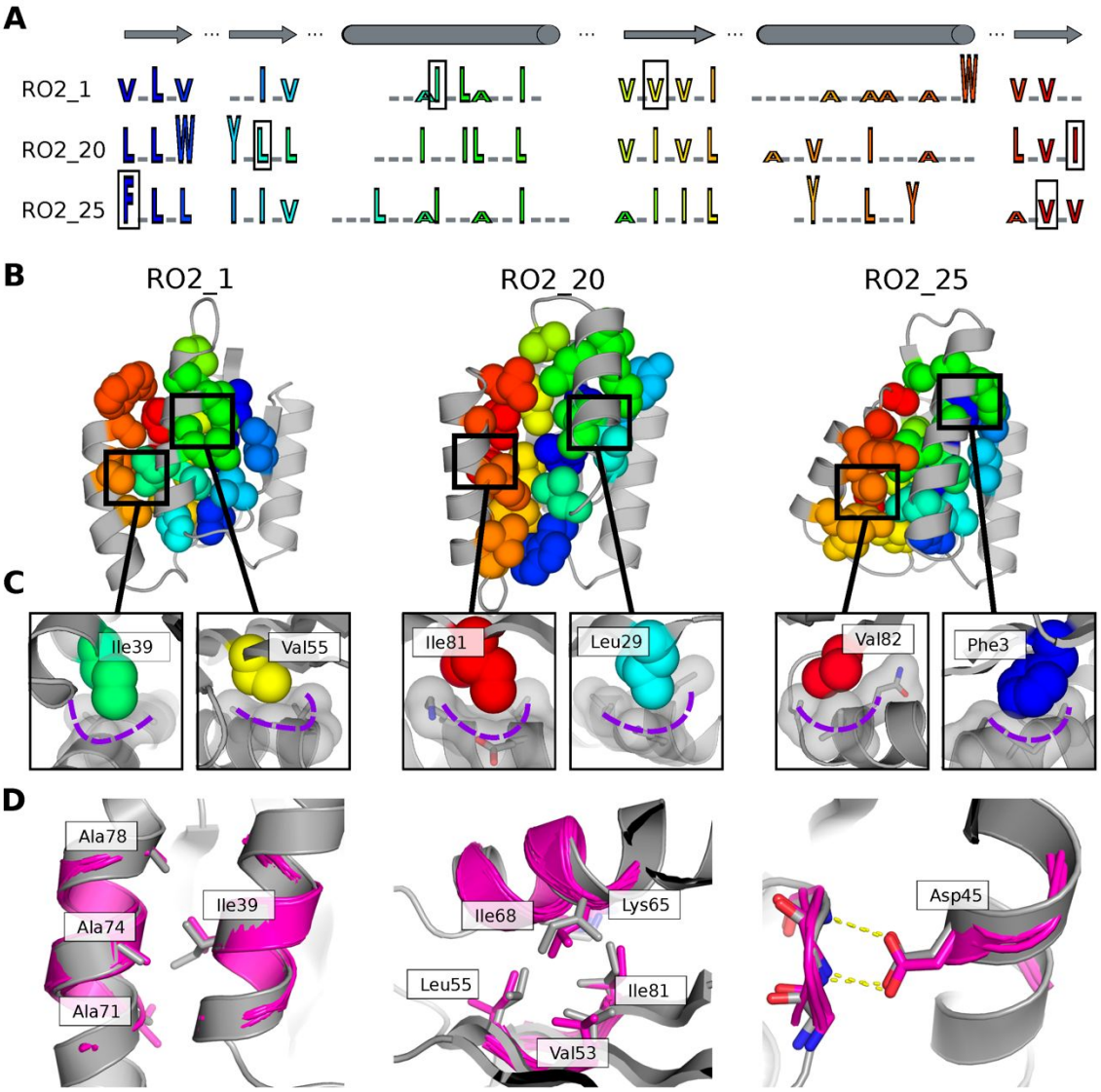

Supplementary Materials for

Expanding the space of protein geometries by computational design of *de novo* fold families

Xingjie Pan, Michael Thompson, Yang Zhang, Lin Liu, James S. Fraser, Mark J. S. Kelly, Tanja Kortemme.

Correspondence to: xingjiepan@gmail.com; tanjakortemme@gmail.com

This PDF file includes:

Materials and Methods

Analysis of native loop-helix-loop (LHL) units in naturally occurring structures

Protein domain structures of all 2737 CATH superfamilies were downloaded from the CATH database (V4.1.0)[1]. Secondary structures for each protein were assigned using the DSSP algorithm[2] integrated in Rosetta[3] and used to identify LHL units in each structure. The number of LHL units in each superfamily was defined as the median number of LHL units in all structures from that superfamily. More than 83% of superfamilies had at least one LHL unit (**Figure S1A**). The LHL units in each superfamily were clustered. Two LHL units were clustered together if they connected the same types of secondary structure elements and the distances between the Cα atoms of their starting and ending residues were within 3 Å. The helix RMSDs (see section: RMSD calculation between helices with different lengths) between all pairs of LHL units in the same clusters are shown in **Figure S1B**.

Generation of loop libraries (**Table S1**)

Each loop library contains loops with a defined length and connecting two secondary structure elements with defined types. Loop libraries were created by scanning the non-redundant protein structure database VALL[4]. All loops in VALL with a given length and connecting defined secondary structure types were selected. Loops were discarded if the helices they connected to had less than 6 residues or the strands they connected to had less than 3 residues. The number of loops in each library was recorded for subsequent redundancy calculation. If a loop had 2 Å or lower backbone heavy atom RMSD with other loops and the

RMSD of the C terminal residues was lower than 1.5 Å, the loop was considered redundant and removed. The redundancy of each loop library was defined as the number of all loops divided by the number of non-redundant loops.

Loop-helix-loop sampling

For each LHL unit to be sampled on a given scaffold structure, two insertion points were chosen as inputs. Residues between insertion points in the input structure were removed. Compatible loops with 2, 3, 4 or 5 residues were selected for each insertion point and inserted. All protein residues were mutated to alanine. Clashes between loop residues and the scaffold were detected. Two heavy atoms were defined to be clashing if the distance between atoms was smaller than the sum of their van der Waals radii times a scale factor of 0.6. Loops that did not clash with the scaffold were kept. All pairs of non-clashing loops were screened to test if a helix can be built to bridge the gap. For each pair of loops, 10-residue helices were grown from each of the ends of the loops using the ideal alpha helix dihedrals (phi=-57°, psi=-47°). The directions of half helices were calculated as the normalized average of all vectors pointing from atom N to atom C of each helix residue. If the dot product of directions of half helices was within 0.5, harmonic angle restraints were applied to the angle formed by the Cα atoms of the helix start residue, front helix break residue and the helix end residue as well as the angle formed by the Cα atoms of the helix start residue, back helix break residue and the helix end residue. Rosetta energy (only omega, rama_prepro and restraint terms were enabled) minimization was applied to minimize the restrained angles to align the two halves of the helix. During the minimization, phi, psi and omega torsions of the LHL unit residues were movable degrees of freedom. After

aligning the helices, if there was a pair of residues on the half helices that had a backbone heavy atom RMSD within 3 Å, the excess residues were trimmed, and Rosetta energy minimization was applied to the LHL unit residue phi, psi and omega torsions to close the gap. During minimization, distances between the atom O and atom H in helix backbone hydrogen bonds as well as angles formed by atom N, atom H and atom O were restrained to maintain the helical structure. Quality filters were applied to the closed helix:

- Rosetta backbone hydrogen bond scores for all reshaped helix residues were lower than -0.7.
- There were no clashes (same definition as above) involving the reshaped helices after mutating all residues to valine (residues were mutated from ALA to VAL to check there was space between backbones for subsequent side chain design).
- The median contact degree (the number of C α atoms within 10 Å from the C α atom of a residue) of helix residues was greater than 1.
- The number of buried unsatisfied hydrogen bonds within the reshaped LHL units was less than 4.

If more than one pair of insertion points was sampled, two LHL units at different insertion points were deemed compatible if there was no clash (same definition as before) between them. A final ensemble of models was produced by applying a group of compatible LHL units at each insertion point. This step resulted in 13,421 models for RO1 designs, 290,836 models for RO2 designs, and 136,683 models for NT designs (**Table S2**). The protocol was developed using PyRosetta[5] and is available at:

https://github.com/Kortemme-Lab/loop_helix_loop_reshaping/releases/tag/1.0.0

The PyRosetta package used in this study was compiled from the Rosetta source code (commit: 3135d32229f5ebd35c8a716af00dcdfbbfa81805).

Sequence design

The spatial positions of residues were defined as the positions of their Cβ atoms (Cα for glycine). The sidechain directions were defined as the vector pointing from the Cα atoms to the Cβ atoms. A residue on the scaffold was defined as pointing toward the reshaped backbone region if there was a residue in the reshaped region such that the cosine of the angle between the vector from the surrounding residue Cα atom to the reshaped residue Cα atom and the sidechain direction vector of the surrounding residue was greater than 0.5. Residues within 10 Å (Cα-Cα distance) from the backbone of the reshaped region and pointing toward the reshaped region were designed (i.e. allowed to change amino acid residue type and rotamer conformation). Residues within 8 Å from any designable residue and pointing toward the designable region were repackable (i.e. allowed to change rotamer conformation but keeping amino acid residue type). Residue types allowed for designable residues were determined by the extent of residue burial using the Rosetta LayerDesign task operation[6]. Cysteine and histidine were disallowed as designable residue types to avoid issues with disulfide bond formation and pH dependency. The Rosetta FastDesign [https://www.rosettacommons.org/docs/latest/scripting_documentation/RosettaScripts/Movers/movers_pages/FastDesignMover] and RotamerTrial [https://www.rosettacommons.org/docs/latest/scripting_documentation/RosettaScripts/Movers/movers_pages/RotamerTrialsMover] protocols were applied to design sequences that stabilize the

backbone structures. The first iteration of design was done using the Dunbrack rotamer library without extra rotamers[7]. 58626, 432735 and 409101 sequences were designed for RO1, RO2 and NT. Designed structures that had less than 2 buried unsatisfied hydrogen bond donors or acceptors, had Rosetta hole scores[8] for the designed residues smaller than 0 and had fragment qualities[9] better than 2 Å were selected for the next iteration of designs. 1163, 9934 and 5715 designs passed the filters for RO1, RO2 and NT. For RO2 and NT, the selected designs were further optimized by 3 repeats of Rosetta FastDesign with extra rotamers enabled by the ex1 and ex2 options in the ExtraRotamersGeneric task operation. 49578 and 22831 sequences were designed for RO2 and NT. Final designs were filtered:

- Fragment qualities for the reshaped regions were better than 1 Å.
- Rosetta hole scores for the designable and repackable residues were lower than 0.
- Rosetta helix complementarity scores (Lawrence and Coleman shape complementarity)[10] for the reshaped helices were better than 0.6.
- There were no buried unsatisfied hydrogen bonds according to the custom buried unsatisfied hydrogen bond filter (next section).
- There were no oversaturated hydrogen bonds, i.e. hydrogen bond acceptors receiving hydrogen bonds from more than the allowed number of donors, for designable and repackable residues.
- The ratio of hydrophobic solvent accessible surface area (SASA) over the total SASA was lower than 58%.

722 and 98 designs passed the filters for RO2 and NT. The custom buried unsatisfied hydrogen bond filter sometimes underestimated the number of buried unsatisfied hydrogen bonds and the

holes filter allowed large hydrophobic holes which can exist in native proteins as binding sites. Therefore, designs that passed the filters with lowest residue average Rosetta scores were examined manually to check for possible issues such as hydrophobic voids and buried unsatisfied hydrogen bonds missed by the automatic filter. For the RO2 designs, we selected 50 top-scoring designs passing these manual criteria.

For the NT designs, we attempted to introduce cavities as potential binding pockets into the protein core. The 98 NT designs that passed the second iteration had hydrophobic cavities because the Rosetta layered design task operation assigned the residues surrounding the cavities to the core layer. We manually selected 10 low energy designs that passed iteration 2 (picking the lowest energy designs that were substantially different from each other) for further sequence design simulations to introduce pockets with polar residues into the proteins. We used the same sequence design protocol as in iteration 2, but with the restriction that 1-3 pocket residues had to be polar residues. For each of the 10 selected designs, 100 new sequences were designed. We then filtered the new designs with the same automatic filters followed by manual inspection as the previous round. 202 designs passed the automatic filters, of which 50 were selected by their Rosetta energy. For each of the 10 designs selected from iteration 2, at least one design derived from it was selected. The sequence design code is available at: https://github.com/Kortemme-Lab/local_protein_sequence_design/releases/tag/1.0.0

Custom buried unsatisfied hydrogen bond filter

The standard Rosetta buried unsatisfied hydrogen bond filter[11] overestimated the number of buried unsatisfied hydrogen bond donors and acceptors in many native structures (**Figure S12**)

because it identified hydrogen bonds based on one static model. However, due to modeling errors and protein conformational flexibility, some of the identified buried unsatisfied hydrogen donors or acceptors present in the models may nevertheless form proper hydrogen bonds. In order to find only the buried unsatisfied hydrogen bond donors or acceptors that cannot be compensated by allowing some conformational flexibility, we developed a structure quality filter called the backrub ensemble consensus buried unsatisfied hydrogen bond (BECBUBH) filter. For each protein residue, except for the N- and C-terminal residues, the BECBUBH filter generated 5 structures by applying a local backrub[12] move on the residues and each of their two neighboring residues. The filter then determined the buried unsatisfied hydrogen bond donors or acceptors for each structure. Only buried unsatisfied donors or acceptors that were consistently present in all 5 structures were recorded. We used the BECBUBH filter to filter designed models.

Ab initio structure prediction

Rosetta *ab initio* structure prediction simulations were run for the top 50 selected designs for each design problem (**Table S2**). Fragments for structure predictions were generated using the make_fragments.pl script[4] distributed with Rosetta. The command for fragment generation was

fragments.pl -verbose -id design_id -frag_sizes 3,9 -n_frags 200 -n_candidates 1000 sequence.fasta

The structures of designs were predicted using the AbinitioRelax application in Rosetta. 20,000 models were generated for each designed sequence. The command was

AbinitioRelax.linuxgccrelease -abinitio:relax -use_filters true -abinitio::increase_cycles 10 -abinitio::rg_reweight 0.5 -abinitio::rsd_wt_helix 0.5 -abinitio::rsd_wt_loop 0.5 -relax::fast -in:file:fasta sequence.fasta -in:file:frag3 fragments_3mer_file -in:file:frag9 fragments_9mer_file -psipred_ss2 ss2_file_from_frag_generation -nstruct num_output -out:sf score_file_output -out:file:silent silent_file_output

For NT designs, standard Rosetta *ab initio* structure prediction simulations failed to sample models sufficiently close to the target model. The target model typically had a significantly lower Rosetta energy than any of the prediction models, indicating a sampling issue. To overcome this problem, we biased *ab initio* structure prediction simulations to favor low RMSD fragments by setting the weight of the score term FragmentCrmsd to be 5 and priority to be 800 in the fragment generation step. We then run standard *ab initio* structure prediction using the biased fragment set. We confirmed that designs folded into the desired target conformation within 1.5 Å when biasing the input fragments used during the structure prediction calculations.

Projecting helices to underlying beta sheets

Models with the Rossmann fold or NTF2 fold were aligned to PDB:2LV8 or PDB:5TPJ, respectively. The 3-dimensional (3D) helix centers were calculated by averaging the C α atom coordinates for all residues in a given helix. The 3D helix directions were defined as the average

of C=O bond directions of the helix residues. The 3D centers and directions were projected onto a 2-dimensional (2D) plane by Cartesian projections. The beta sheet peptide bonds were shown as parallelograms where the Cα atoms were located at the center of horizontal edges.

Binning the helix geometry space

Each helix was assigned a 6-dimensional vector whose first 3 coordinates were the helix center position and the last 3 coordinates were the direction of the helix. As above, the center of a helix was the average of the Cα atom coordinates. The direction was the average of C=O bond directions normalized to a unit vector. The Cartesian space of helix centers was divided into 2Å cubes and the directions were divided into 8 octants. A 6-dimensional bin was assigned to a helix based on the cube and octant that the helix belonged to.

RMSD calculation between helices with different lengths

To calculate RMSD between two helices with different lengths, the longer helix was truncated. Only the middle part of the longer helix that had the same length as the shorter helix was kept. RMSDs between the corresponding backbone heavy atoms (N, Cα and C) were calculated.

TM-align analysis

The designed models were submitted to the COFACTOR server[13], which used TM-align to find the 10 closest structures from the PDB. Except for the design RO2_5, the PDB structure 2KPO is the closest structure for all Rossmann fold designs and it ranked 2nd for the design

RO2_5. The PDB structure 5TPJ is the closest for all NTF2 fold designs. The difference between the designed geometries and known structures was then quantified by calculating the RMSD between the designed helices and the corresponding helices on the closest known structures with the same topologies found by TM-align (**Fig. 3A**).

Analysis of tertiary structure motifs

Tertiary structure motif analysis was performed using the MASTER[14] program. Small pieces of tertiary structures were specified manually from the well folded designs. The tertiary pieces included designed loops and fragments of interacting secondary structure elements involving the backbone reshaped regions (**Figure S11**). The helical element sizes were between 1 to 2 turns (5-9 residues) and the strand element sizes were between 3 to 5 residues. The tertiary pieces were extracted from the design models and saved as query pdb files. The query pdb files were converted to MASTER input query (pds) files by

createPDS --type query --pdb query.pdb

The query structures were searched against the standard MASTER database with

master --query query.pds --targetList MASTER/database/list --rmsdCut 0.5 --matchOut query.match --seqOut query.seq --bbRMSD --structOut query.struct

Protein expression tests

Plasmids (pET-28a(+)) encoding the designed proteins were ordered from Twist Bioscience. The DNA sequences of the designed proteins were inserted between the NdeI and XhoI restriction sites, which added the DNA coding sequence for an N-terminal MGSSHHHHHHSSGLVPRGSHM tag to the designed proteins. The plasmids were transformed into *Escherichia coli* BL21(DE3) cells. Proteins were expressed by overnight cell culture in 5mL autoinduction medium (ZY medium, 10 g/L tryptone, 5 g/L yeast extract) supplemented with the following stock mixtures: 20xNPS (1M Na_2HPO_4, 1 M KH_2PO_4, and 0.5 M $(NH_4)_2SO_4$), 50x 5052 (25% glycerol, 2.5% glucose, and 10% α-lactose monohydrate), 1000x trace metal mixture (50 mM $FeCl_3$, 20 mM $CaCl_2$, 10 mM each of $MnCl_2$ and $ZnSO_4$, and 2 mM each of $CoCl_2$, $CuCl_2$, $NiCl_2$, Na_2MoO_4, Na_2SeO_3, and H_3BO_3 in 60 mM HCl))[15] with 50 μg/ml kanamycin at 37°C. Cell cultures were aliquoted into 1mL aliquots. Cells were spun down by centrifuging at 20,000 g for 3 min. Cell pellets were resuspended in 1mL Phosphate-buffered saline (PBS) buffer (8g/L NaCl, 0.2g/L KCl, 1.44g/L Na_2HPO_4, 0.24g/L KH_2PO_4, pH=7.4) and lysed by sonication. Soluble and insoluble parts were separated by centrifuging at 21,000 g for 5 minutes. The solubility of a designed protein was assessed by Coomassie-stained SDS-PAGE (BIO-RAD Cat. #456-1095).

Protein expression and purification

Plasmids encoding the N-terminally His-tagged designed proteins were transformed into *Escherichia coli* BL21(DE3) cells. Colonies were inoculated into 5mL LB medium and cultured at 37°C for 12 hours. Seed cultures were inoculated into 1 L autoinduction medium and cultured at 225 RPM shaking speed at 37°C overnight. Cell cultures were centrifuged at 5,000 g for 5

minutes to spin down the cells. Cell pellets were resuspended in 30mL equilibration buffer (50mM Tris pH=7.5, 300mM NaCl, 10 mM imidazole) and lysed using a microfluidizer. Cell lysate was centrifuged at 39,000 g for 30 minutes to separate the soluble and insoluble fractions. The soluble fraction was mixed with 1mL Ni-resin beads (Thermo Scientific #88222) to pull down the His-tagged proteins. Ni-resin beads were washed 3 times with the wash buffer (50mM Tris pH=7.5, 300mM NaCl, 25mM imidazole). Proteins were eluted 3 times with 1mL elution buffer (50mM Tris pH=7.5, 300mM NaCl, 250mM imidazole). For crystallization, His-tags were cleaved by 10 NIH unit bovine thrombin (Sigma-Aldrich T4648-10KU) overnight at room temperature. Then the samples were further purified using a HiLoad® 16/600 Superdex® 75 pg size exclusion column (GE) with PBS buffer. The monomeric fraction was collected for subsequent characterization.

Analytical size exclusion chromatography

Protein samples purified by His-tag pull down (if sufficiently pure) or after additional purification with the HiLoad® 16/600 Superdex® 75 pg size exclusion column were analyzed using a Superdex® 75 10/300 GL size exclusion column from GE with PBS buffer. The relation between elution time and log molecular weight was fitted using a linear regression model with the BioRad Gel Filtration Standard (Catalog #151-1901).

Circular dichroism spectroscopy

Circular dichroism (CD) data were collected on a Jasco J-710 spectrometer. Purified RO1 proteins were diluted into 50mM phosphate buffer (pH 7.0). Purified RO2 and NT proteins were

diluted into PBS buffer (8g/L NaCl, 0.2g/L KCl, 1.44g/L Na_2HPO_4, 0.24g/L KH_2PO_4, pH=7.4). The concentrations of diluted samples ranged from 2μM to 5μM. Protein concentrations were determined using the absorbance at 280 nm using a NanoDrop (Thermo Scientific). CD spectra were measured using a 1mm cuvette at 25°C. Melting curves at 220nm were measured by increasing temperature from 25°C to 95°C using a rate of 1°C/min.

1D-^{1}H NMR spectra

Purified proteins were exchanged into 50mM phosphate buffer (pH 7.0). Samples were concentrated to 15-200 μM. 56 mL D_2O was added to 500 mL samples such that the final volume had 10% D_2O and 90% H_2O. The 1D 1H spectra (pulse program: zgesgp) were measured at 297.9 K using a Bruker Avance I 800 MHz spectrometer with a Z-gradient TXI cryo-probe. The temperature was calibrated with 4% MeOD using the following coefficients of T (K) = (4.109 - D) * 0.008708 where D is the chemical shift difference between the CH_3 and OH protons in methanol. The spectra were processed with the program NMRPipe[16].

Protein expression for NMR structure determination

^{15}N and ^{13}C labeled proteins were expressed by growing *E. coli* in M9 minimal medium that included ^{13}C-glucose and $^{15}NH_4Cl$ (6g/L Na_2HPO_4, 3g/L KH_2PO_4, 0.5g/L NaCl, 0.5g/L $^{15}NH_4Cl$, 50mg/L EDTA, 8.3mg/L $FeCl_3$ x 6 H_2O, 0.84mg/L $ZnCl_2$, 0.13mg/L $CuCl_2$ x 2 H_2O, 0.1mg/L $CoCl_2$ x 6 H_2O, 0.1mg/L H_3BO_3, 0.016mg/L $MnCl_2$ x 6 H_2O, 0.2% (w/v) ^{13}C-glucose, 1mM $MgSO_4$, 0.3mM $CaCl_2$, 1mg/L Biotin, 1mg/L Thiamine). Single bacterial colonies were first inoculated into 5mL seed culture and grown at 37 °C overnight. The seed culture was inoculated

into 1L ^{15}N ^{13}C labeled M9 minimal medium and grown at 37 °C until OD_{600} reached 0.5-0.7. Then 1mL 1M IPTG was added to induce protein expression at 18 °C overnight. The expressed proteins were purified following the Ni-resin pull down protocol described in the protein purification section. The His-tag purified proteins were further purified using the HiLoad® 16/600 Superdex® 75 pg size exclusion column from GE with 50mM phosphate buffer at pH 7.0. The monomeric fractions were collected and concentrated to 0.5-1 mM for NMR experiments.

Structure determination by NMR

Proteins labeled with ^{15}N and ^{13}C were exchanged into 50mM phosphate buffer (pH 7.0). 10% D_2O was added to samples and the final protein concentrations were 0.74-0.8 mM. NMR spectra were measured at 297.9 K. Two dimensional (2D) ^{15}N-HSQC (pulse program: fhsqcf3gpph), 2D ^{13}C-HSQC (pulse program: hsqcetgpsisp2), 16 ms 3D HCCH-TOCSY (pulse program: hcchdigp3d) and 120 ms 3D simultaneous $^{13}C/^{15}N$-NOESY-HSQC (pulse program: noesyhsqcgpsismsp3d) spectra were measured using a Bruker Avance I 800 MHz spectrometer with a Z-gradient TXI cryo-probe. 3D CACB(CO)NH (pulse program: hncocacbgpwg3d) and 3D CACBNH (pulse program: hncacbgpwg3d) spectra were measured using a Bruker Avance DRX500 spectrometer with a Z-gradient QCI cryo-probe at 297.6 K (same temperature calibration as described above). NMR spectra were processed using the program NMRPipe[16] and indirect referencing to an external DSS standard was used[17]. Resonances were assigned using the program CCPN Analysis[18]. Backbone resonances were assigned using the 2D ^{15}N-HSQC, 3D CACB(CO)NH and 3D CACBNH spectra. Sidechain resonances were assigned using the 2D

^{13}C-HSQC and 3D HCCH-TOCSY spectra. Distance restraints were generated using CCPN Analysis. Dihedral restraints were generated using the program DANGLE[19]. Hydrogen bond restraints included in the structure calculations were based on secondary structures predicted by DANGE and nOe patterns typical of alpha-helical secondary structure. The programs ARIA version 2.3.2[20] and CNS version 1.2 .1[21] were used to calculate the NMR structures. To solve the structures, 9 iterations of simulated annealing were performed using CNS. For the first 8 rounds of simulated annealing, the n_structures parameter was set to 100 and the n_best_structures parameter was set to 35. For the 9th round, the n_best_structures parameter was set to 20. Finally, a refinement in water was performed on the 20 structures from the 9th iteration. Otherwise, the default values were used for the remaining ARIA parameters. The ensemble of the refined structures was validated using the PDB validation server[22] and the Protein Structure Validation Suite (PSVS) server[23]. The agreement between structures and NMR data were assessed using the program PyRPF[24] integrated into the CCPN suite.

Protein crystallization

We concentrated the NT_9 protein to 25.2 mg/mL in buffer containing 20 mM Tris Buffer (pH=7.5) and 150 mM sodium chloride, and carried out initial crystallization trials using the JCSG I-IV commercial crystallization screen (Qiagen). Crystallization drops were prepared in 96-well sitting drop format by mixing 100 nl of protein solution with 100 nl of the mother liquor using a Mosquito liquid handling robot (TTP Labtech). Drops were sealed inside a reservoir containing an additional 100 µl of the mother liquor solution. Crystals were obtained from mother liquor containing 0.1M MES Buffer at pH=6, 30% PEG-600, 5% PEG-1000, and

10% Glycerol. Crystals from the initial screen were used for data collection without further optimization.

X-ray data collection and processing

Prior to X-ray data collection, crystals were flash-cooled by rapid plunging into liquid nitrogen. The high concentrations of polyethylene glycols and glycerol in the crystallization mother liquor allowed the crystals to be harvested and frozen directly without additional cryoprotection. We collected single-crystal X-ray diffraction data on beamline 8.3.1 at the Advanced Light Source. The beamline was equipped with a Pilatus3 S 6M detector (Dectris), the X-ray energy was set to 11111 keV, and the crystals were maintained at a cryogenic temperature (100 K) throughout the course of data collection.

We processed the X-ray data using the Xia2 system[25], which performed indexing, integration, and scaling with XDS and XSCALE[26], followed by merging with Pointless[27]. A resolution cutoff (1.50 Å) was taken where the completeness of the data fell to a value of approximately 90%. Although other metrics of data quality (such as CC1/2 and $<I/\sigma I>$) suggest that a more aggressive resolution cutoff would be acceptable, we were limited by the data completeness that could be obtained with the minimum accessible sample-to-detector distance. Further information regarding data collection and processing is presented in Table S5. The reduced diffraction data were analyzed with phenix.xtriage (http://www.ccp4.ac.uk/newsletters/newsletter43/articles/PHZ_RWGK_PDA.pdf) to check for common crystal pathologies, none of which were identified.

Structure determination

We obtained initial phase information for calculation of electron density maps by molecular replacement using the program Phaser[28], as implemented in the PHENIX suite[29]. We identified a single copy of the protein in the asymmetric unit using the coordinates from our design model, consistent with an analysis of Matthews probabilities for the observed unit cell and molecular weight of the protein[30,31].

Next, we attempted to rebuild our model of the protein using the electron-density maps calculated using the model phases derived from molecular replacement. We immediately noticed that a cavity in the protein surface, inherent to the designed topology, was occupied with a large electron density feature present in both 2mFo-DFc and mFo-DFc electron density maps. This feature was interpreted as phosphatidylethanolamine, an *E. coli* phospholipid that we suspect binds to the protein during recombinant expression and remains bound throughout the purification. In addition to modeling the bound phospholipid, we rebuilt parts of the design model using the initial electron-density maps calculated from molecular replacement. We then performed additional, iterative refinement of atomic positions, individual atomic displacement parameters (B-factors) with a TLS model, and occupancies, using riding hydrogen atoms and automatic weight optimization, until the model reached convergence. Our tentative modeling of phosphatidylethanolamine bound to the protein was supported by the overall flatness of mFo-DFc electron density maps in the vicinity of the ligand, and by the reduction in R-free obtained when adding the ligand to the model. All model building was performed using Coot[32]

and refinement steps were performed with phenix.refine (v1.16-3549) within the PHENIX suite[29,32]. Restraints for the phosphatidylethanolamine (PEE) ligand were calculated using phenix.elbow[33]. The final model coordinates were deposited in the Protein Data Bank (PDB[34]) under accession code 6W90. Further information regarding model building and refinement is presented in **Table S5**.

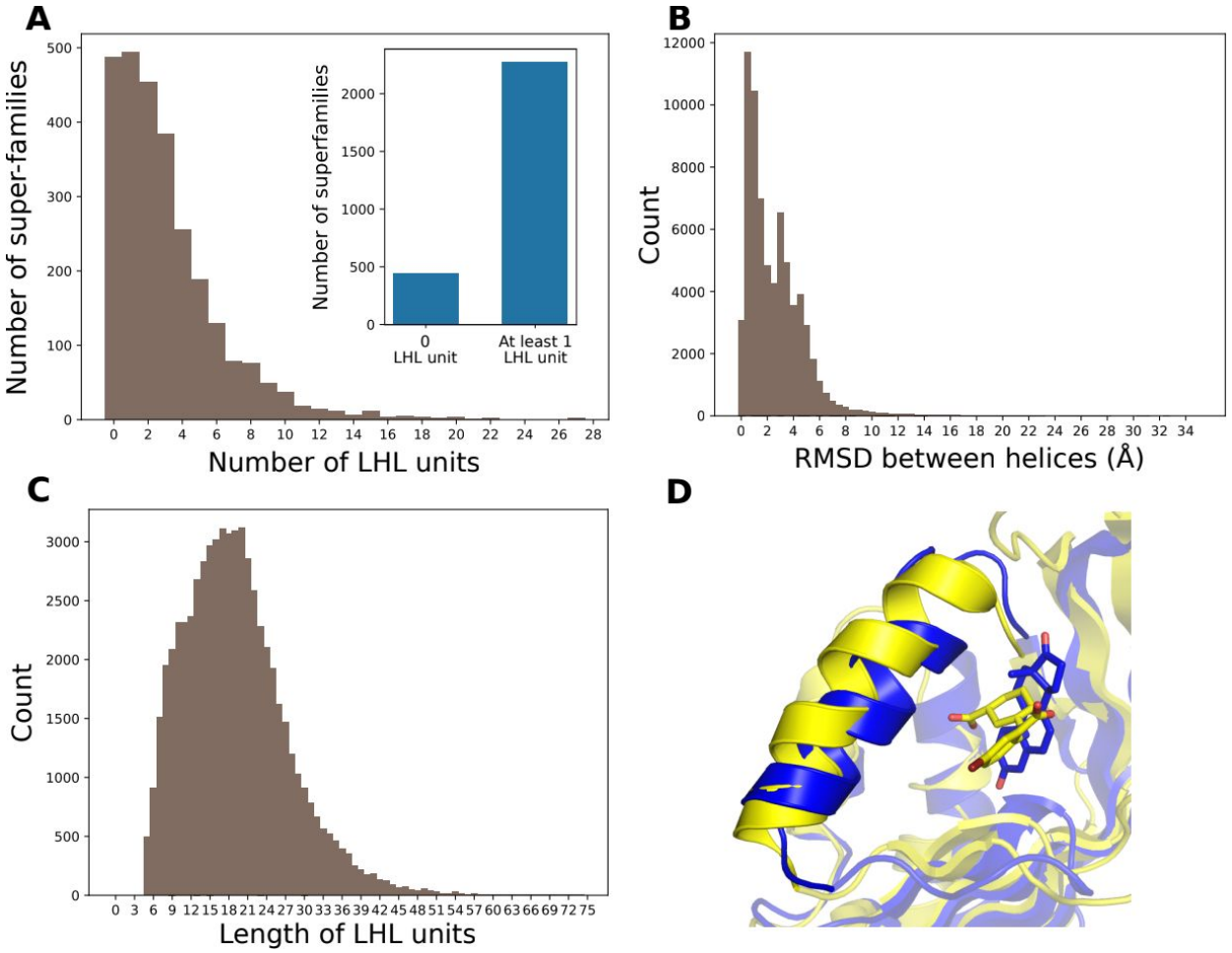

Fig. S1. Diversity of geometries in naturally occurring fold topologies to enable distinct functions.

A. Distribution of the number of LHL units contained in each CATH protein superfamily. Inset: numbers of superfamilies that have no or at least one LHL units. 83.7% of all CATH superfamilies have at least one LHL unit. **B.** Diversity of the geometries of LHL units in CATH superfamilies. Shown are the helix RMSDs between all pairs of LHL units in the same clusters computed as described in Supplementary Methods. **C.** Distribution of LHL lengths in all CATH structure superfamilies. **D.** Example where a change of the LHL geometry at the active site alters ligand specificity. The blue LHL element is from ketosteroid isomerase (PDB:1OH0) that binds a equilenin and the yellow LHL element is from Phenazine biosynthesis protein A/B that binds a 5-bromo-2-{[(1S,3R)-3-carboxycyclohexyl]amino}benzoic acid (PDB:3JUM).

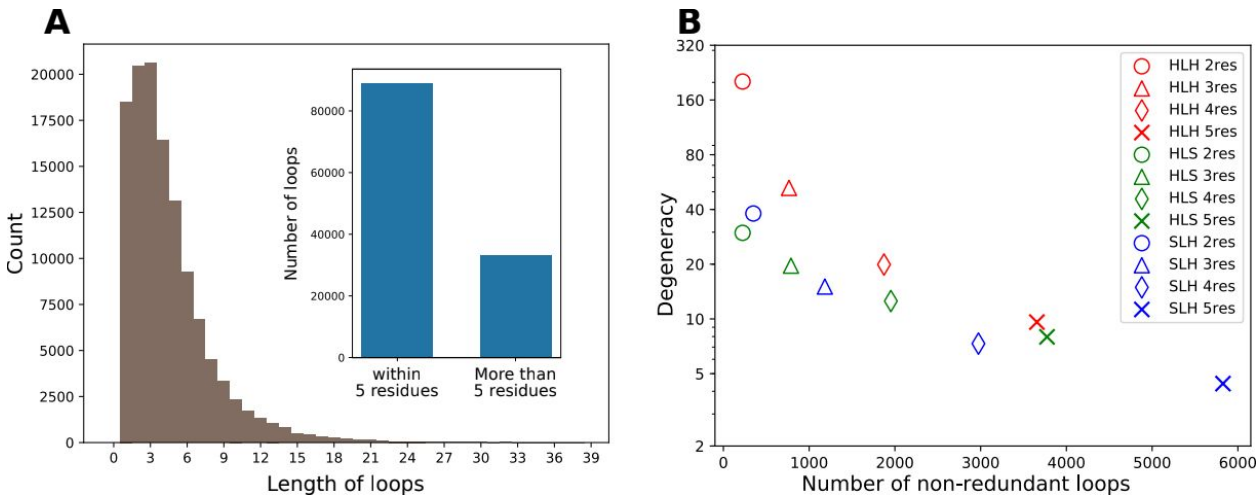

Fig. S2. Common loop connector elements in naturally occurring LHL units.

A. Distribution of loop lengths in LHL units. Inset: numbers of loops that have at most 5 residues or more than 5 residues. **B.** Sizes of non-redundant loop libraries versus the degeneracy defined as the total number of loops divided by the number of non-redundant loops. Loops connecting two helices are shown in red. Loops connecting a helix and a strand are shown in green. Loops connecting a strand and a helix are shown in blue. Loops with different numbers of residues are indicated by different markers.

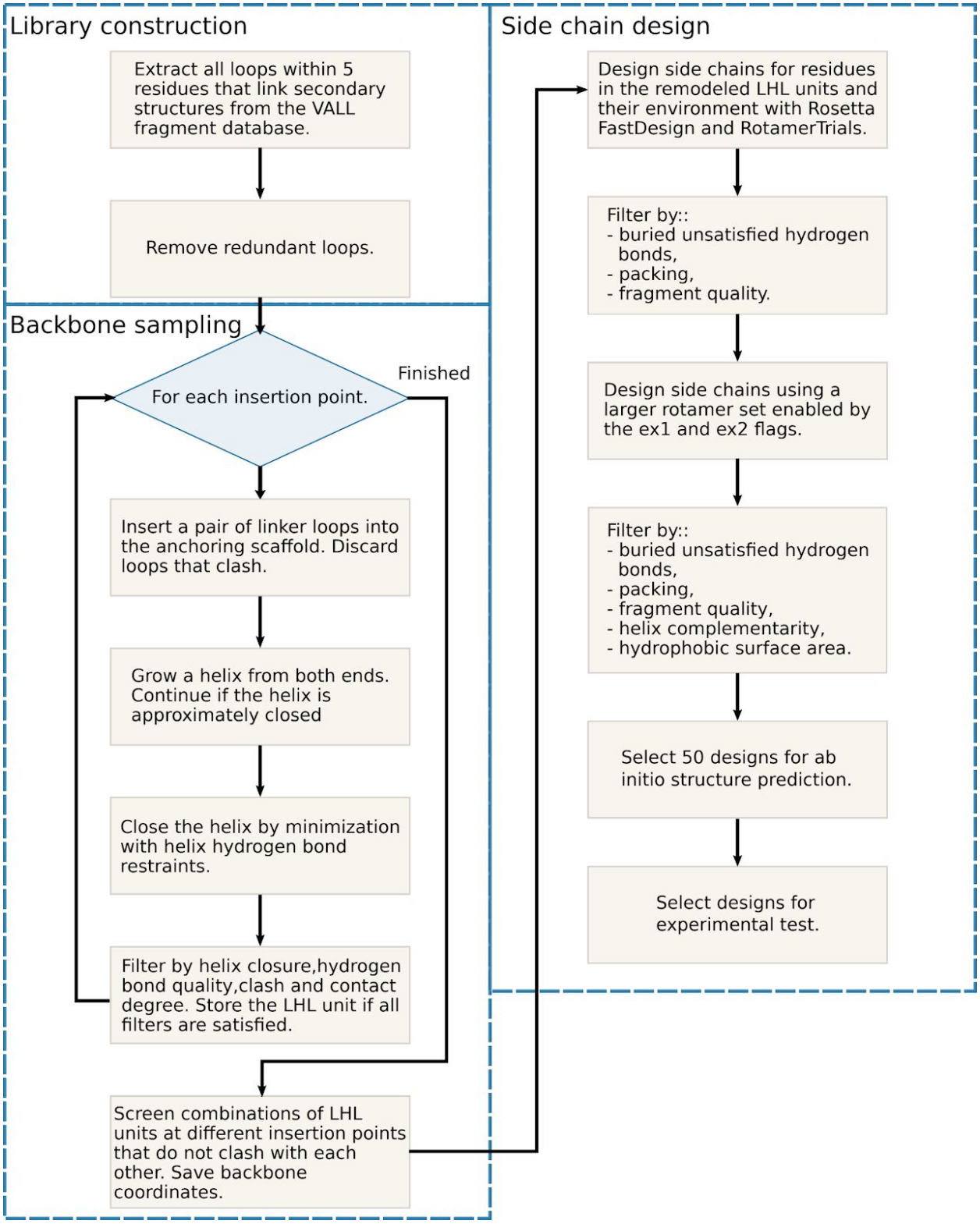

Fig. S3.

Detailed flowchart of the LUCS design protocol.

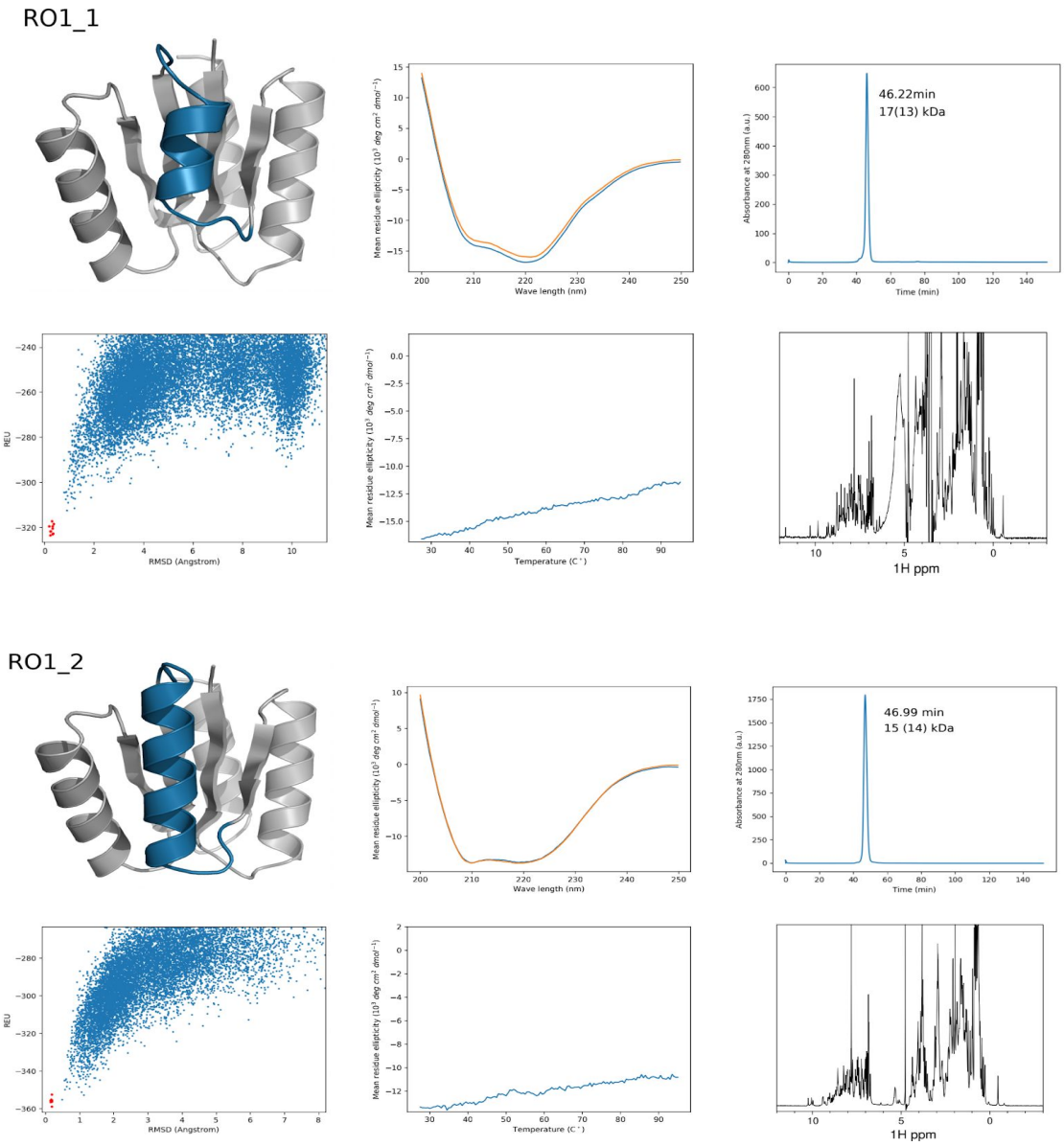

Fig. S4. Characterization of well-folded designs. For each design, the design model is shown in the upper left panel with the reshaped LHL units shown in blue. The lower left panels show the results of Rosetta *ab initio* structure prediction simulations. Each blue point represents a model from the prediction simulations and each red point represents a relaxed design model. For the NTF2 fold designs, the *ab initio* structure prediction simulations used a biased fragment set (see Supplementary Methods). The upper middle panels are the CD spectra at 25°C before (blue) and after measuring a melting curve (orange). The lower panels are CD melting curves measured at 220nm. The upper right panels show the size exclusion chromatograms. The peak positions and molecular weights calculated from peak positions (molecular weights calculated from amino acid sequences) are shown next to the monomer peak. For designs RO1_8, RO1_9, RO2_5, RO2_6, RO2_9, RO2_10, RO2_20 and RO2_25, the chromatograms were measured using samples purified by gel filtration. The chromatograms for the remainder of the designs were

measured directly after His-tag purification. The lower right panels show the 1D-1H NMR spectra.

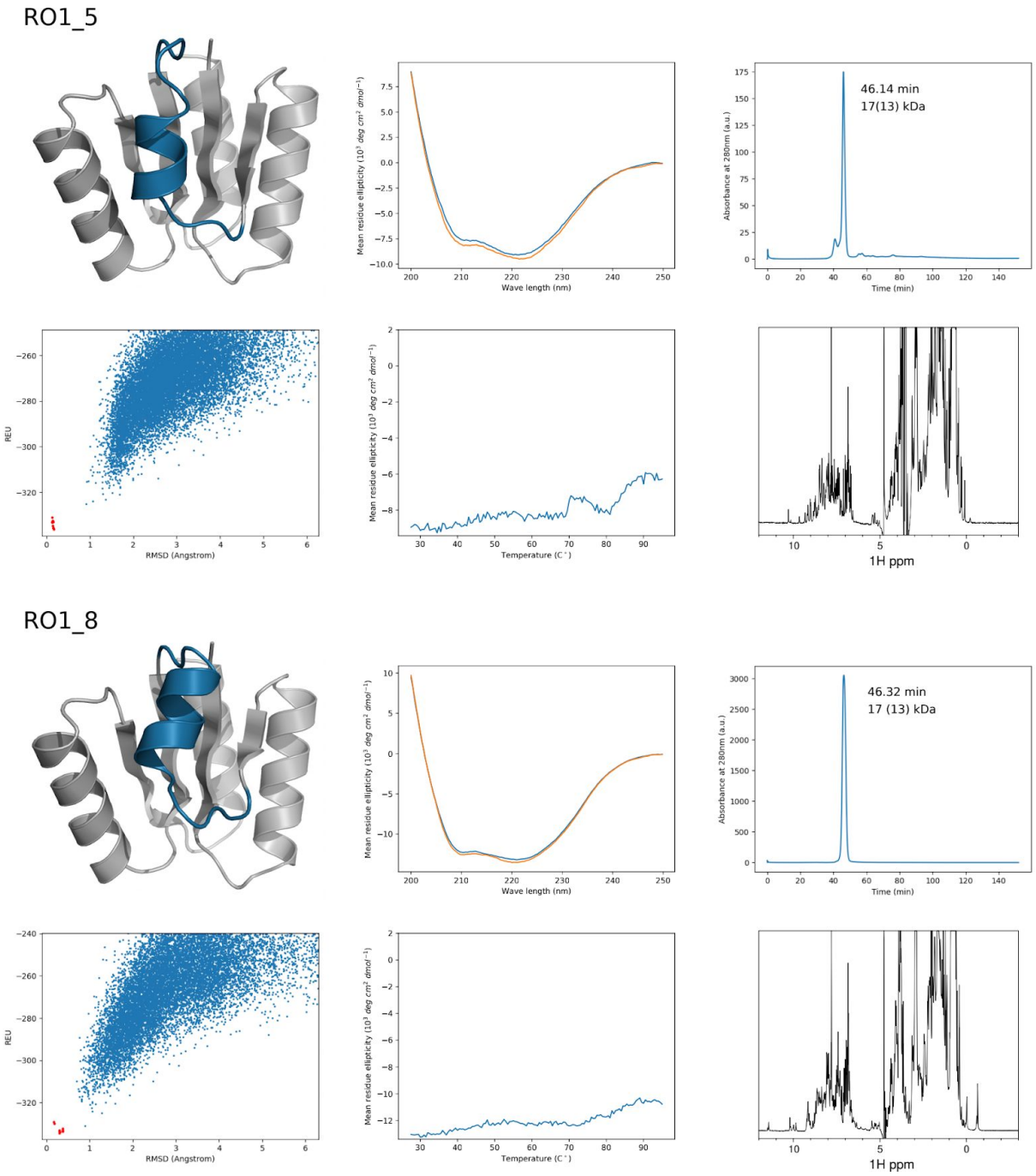

Fig. S4. Characterization of well folded designs cont.

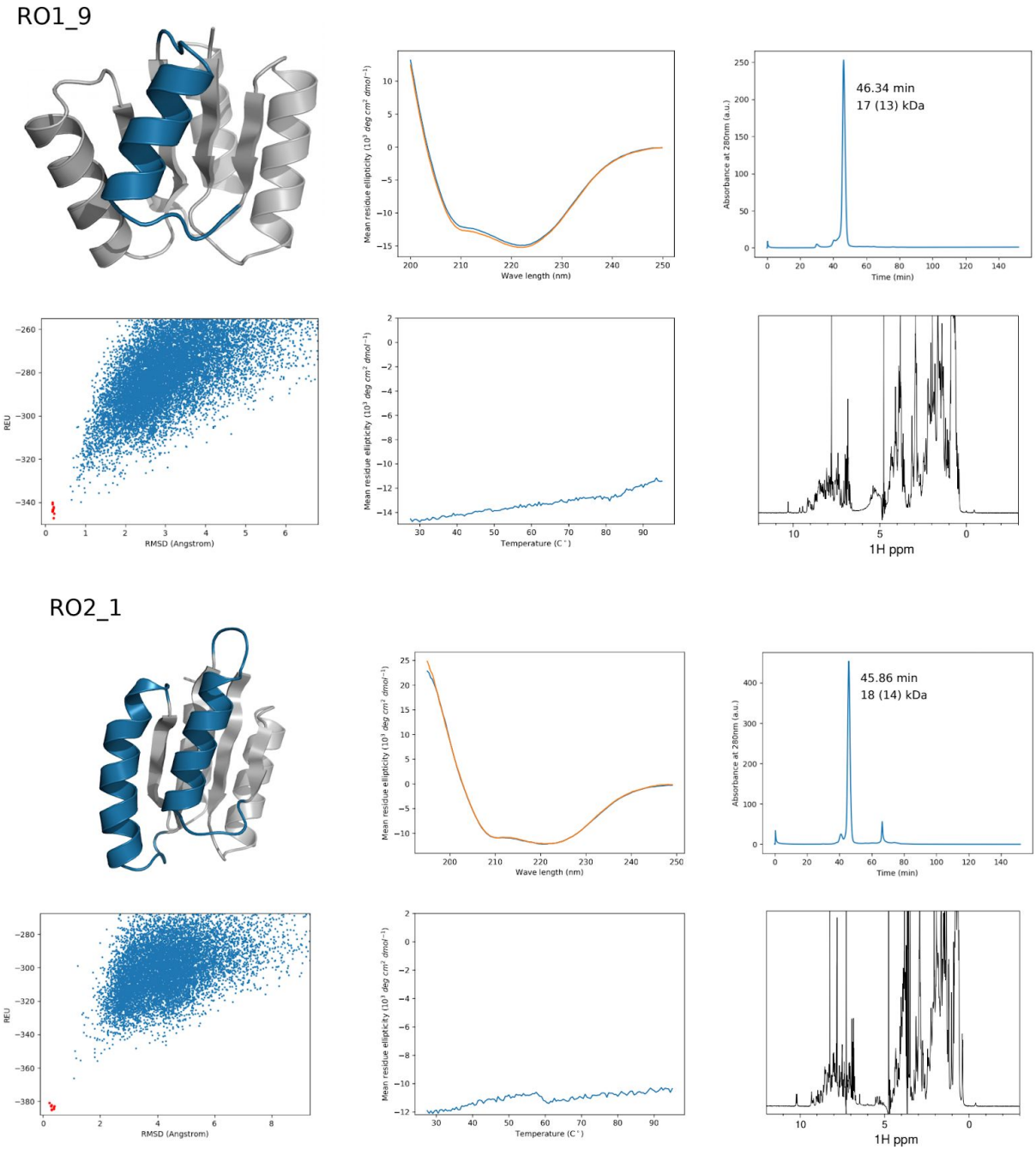

Fig. S4. Characterization of well folded designs cont.

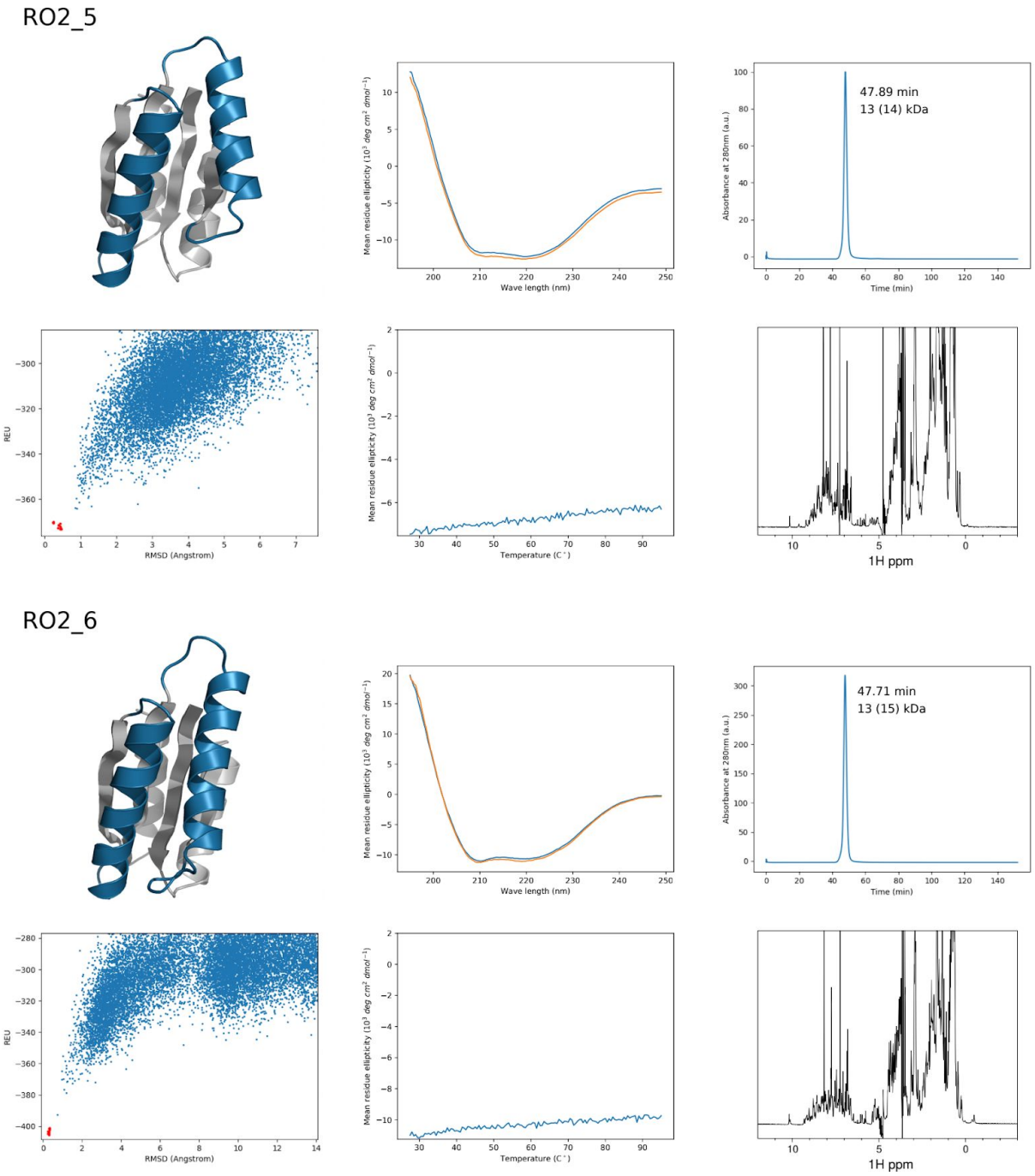

Fig. S4. Characterization of well folded designs cont.

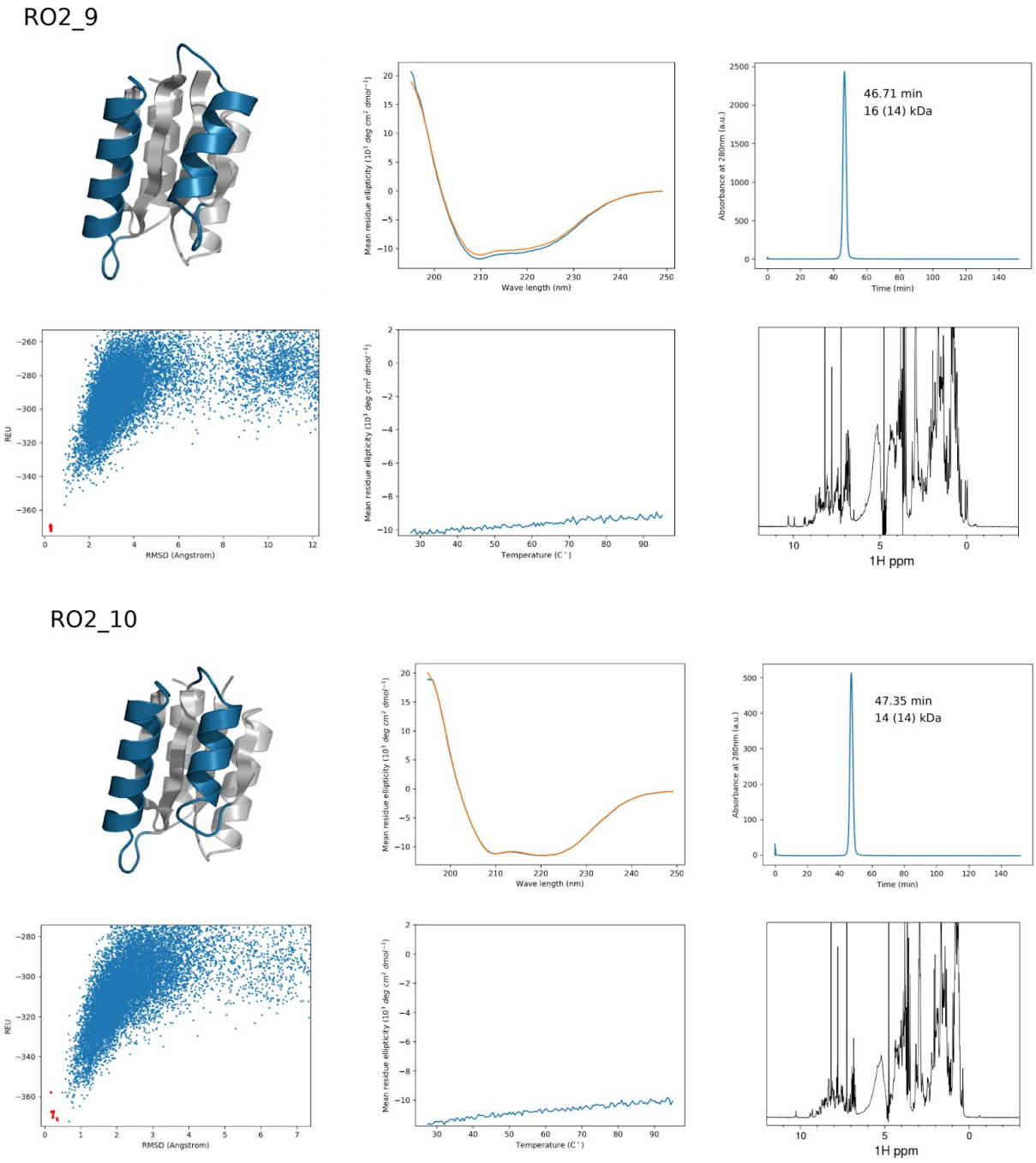

Fig. S4. Characterization of well folded designs cont.

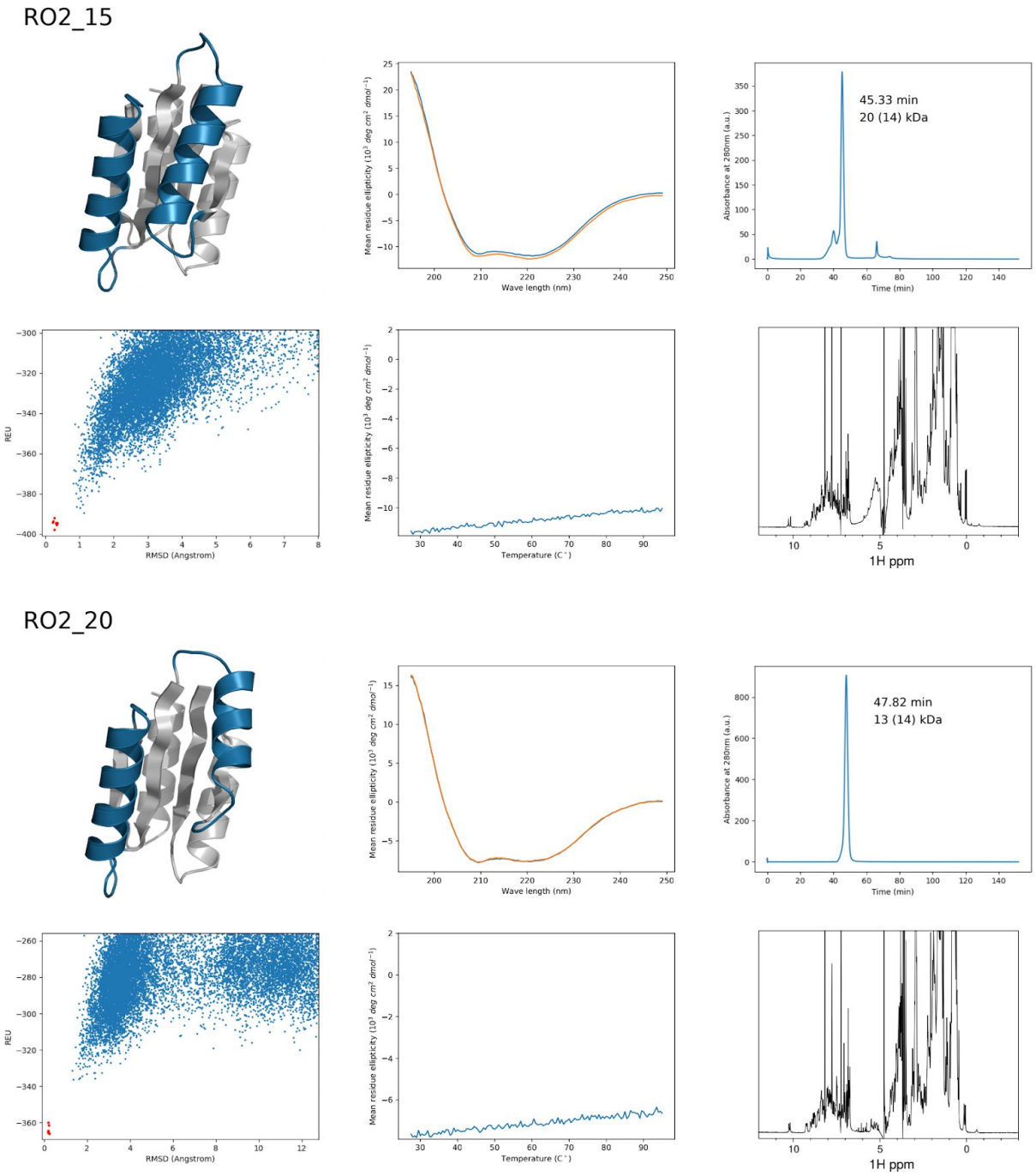

Fig. S4. Characterization of well folded designs cont.

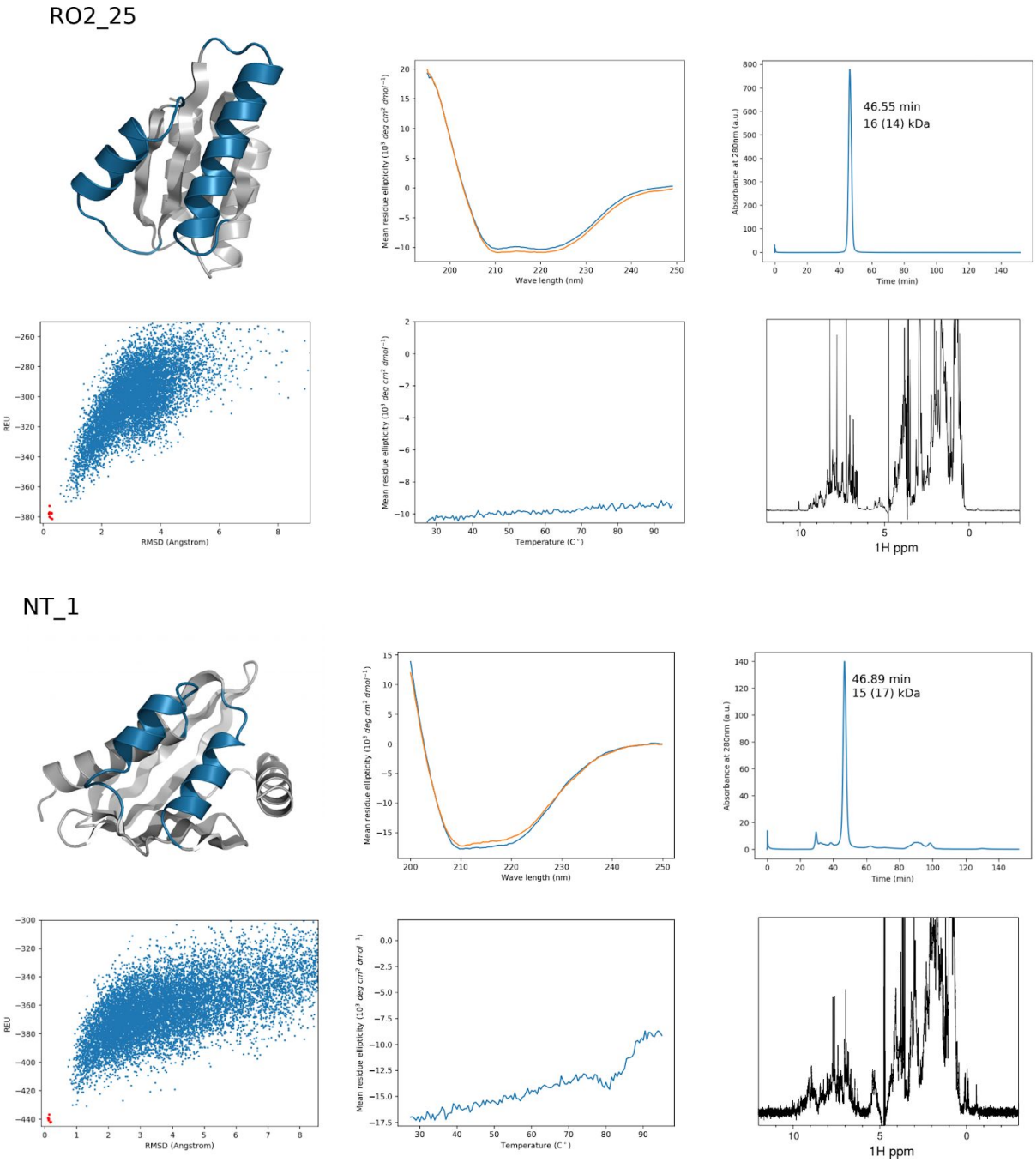

Fig. S4. Characterization of well folded designs cont.

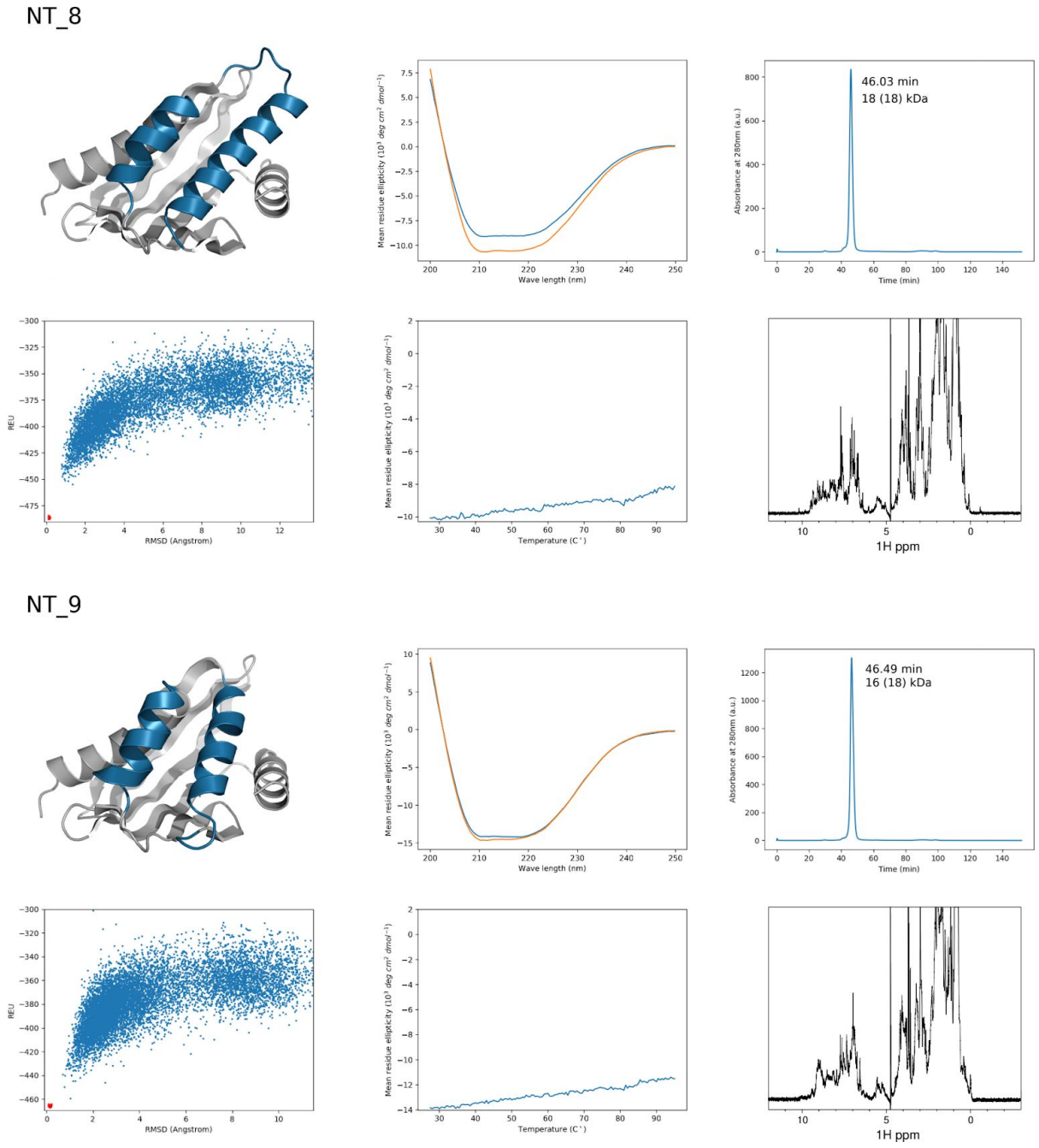

Fig. S4. Characterization of well folded designs cont.

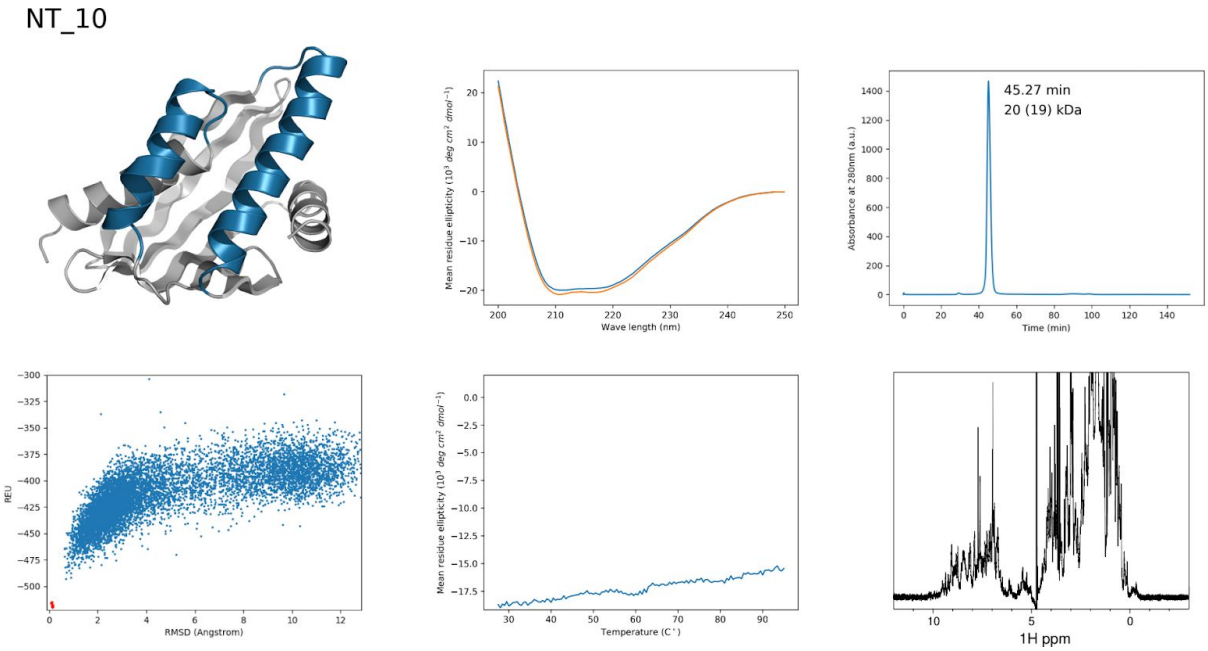

Fig. S4. Characterization of well folded designs cont.

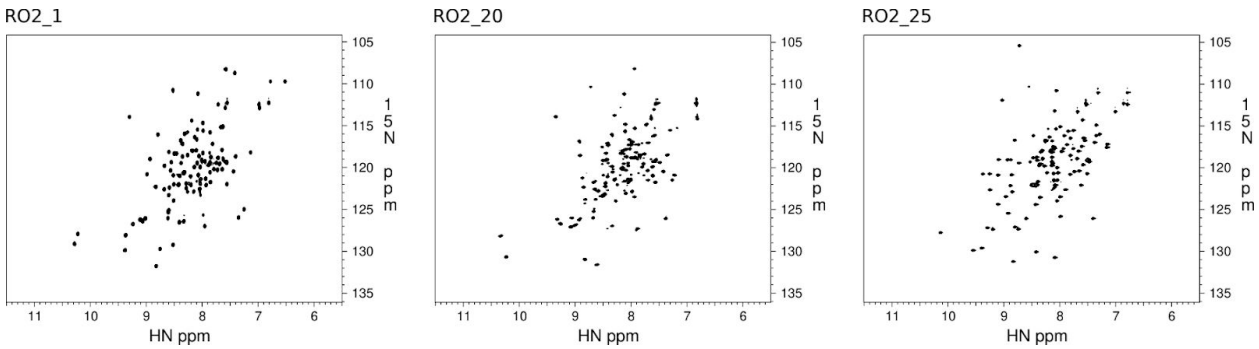

Fig. S5. ^{15}N-^{1}H HSQC spectra of designs whose structures were solved by NMR.

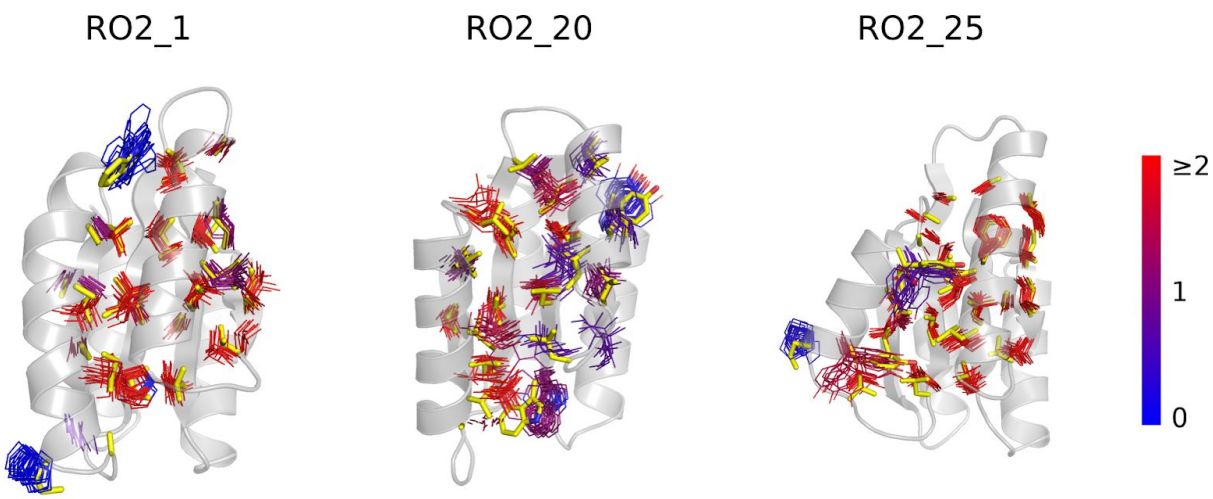

Fig. S6. Conformations of core side chains overall agree between designed models and structures solved by NMR. The backbones of the designed models are shown as cartoons. The hydrophobic core side chains of models are shown as yellow sticks. The conformations of the side chain in the NMR models are shown as lines and colored according to the ratio of the number of long range (distance in primary sequence larger than 3) NOEs involving its side chain atoms over the number of its side chain atoms.

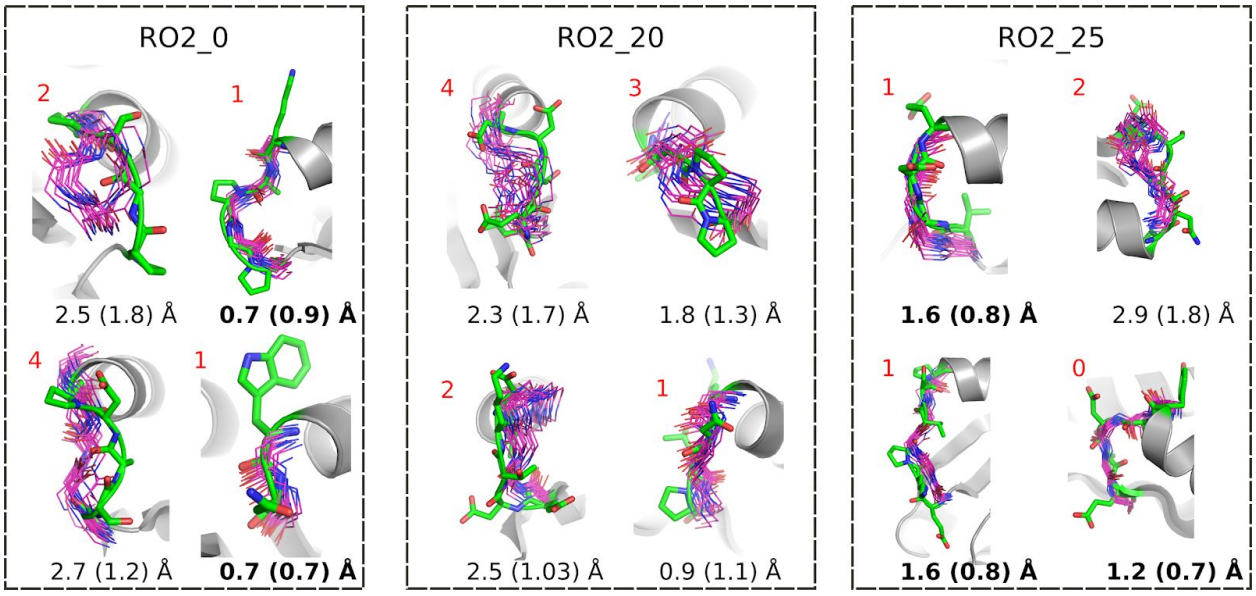

Fig. S7. Comparison of loop conformations between designed models and structures solved by NMR. The loops of designed models are shown as green sticks. The backbone heavy atoms of experimentally solved loops are shown in magenta. The backbone heavy atom RMSDs between the designs and lowest energy NMR models are shown below each loop and the max loop residue ensemble backbone RMSDs calculated by CCPN analysis are shown in parentheses. The 5 converged loops (pairwise backbone RMSD within the ensemble of NMR models within 1 Å) have RMSDs within 1.6Å (shown in bold). The number of residues that lack long range (distance in primary sequence larger than 3) NOE restraints are shown at the top left of each loop (red).

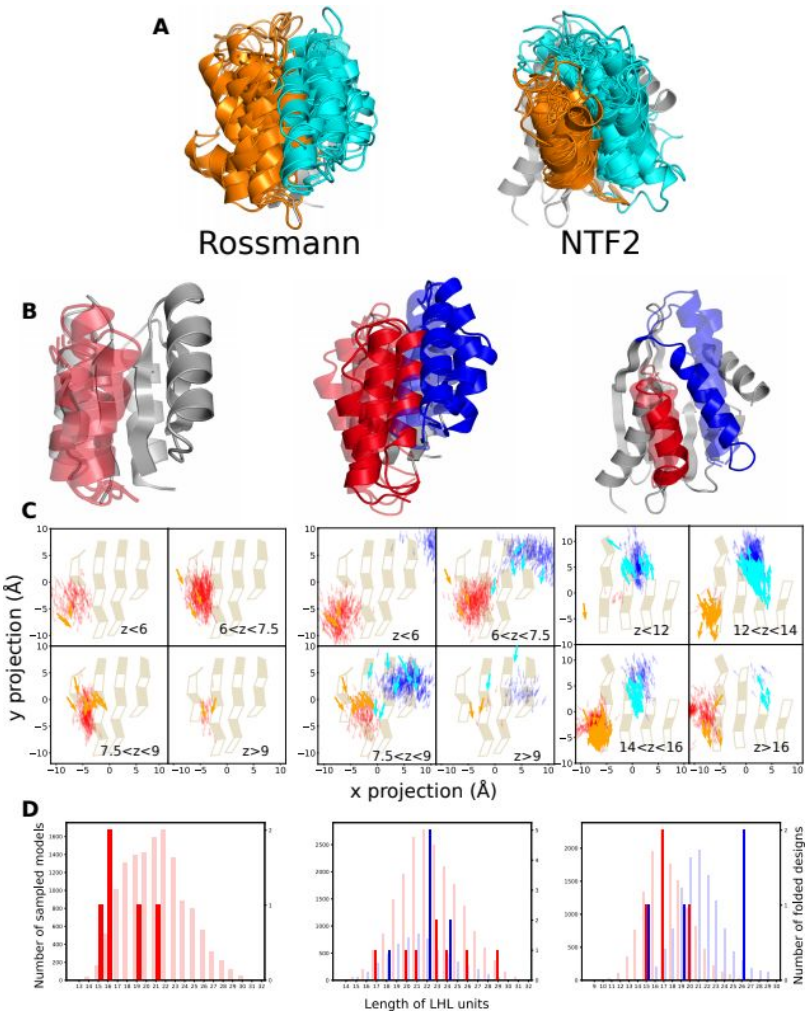

Fig. S8. Distributions of LHL geometries in designed *de novo* fold families. **A.** Structures of native Rossmann fold (left) and NTF2 fold (right) proteins (the two helices corresponding to the designed regions are shown in orange and cyan). The Rossmann fold structures are from the CATH superfamily 3.40.50.1980 and the NTF2 fold structures are from the CATH superfamily 3.10.450.50. In **B**,**C** and **D**, columns show the 3 design problems: Left, Rossman fold with one designed LHL unit; middle, Rossmann fold with two designed LHL units; right: NTF2 fold with two designed LHL units. **B.** Superimposition of well-folded designs. The designed LHL units are colored in red or blue. Designs with experimentally solved structures are shown in solid colors and all other well-folded designs are shown in transparent colors. **C.** Projection of centers and directions of helices from designable LUCS models (red, blue) and known structures (orange, cyan) onto the underlying beta sheets, as shown in **Fig.3** in the main text but overlaid. **D.** The distributions of LHL lengths of the sampled models (light colors) and the well-folded designs (dark colors).

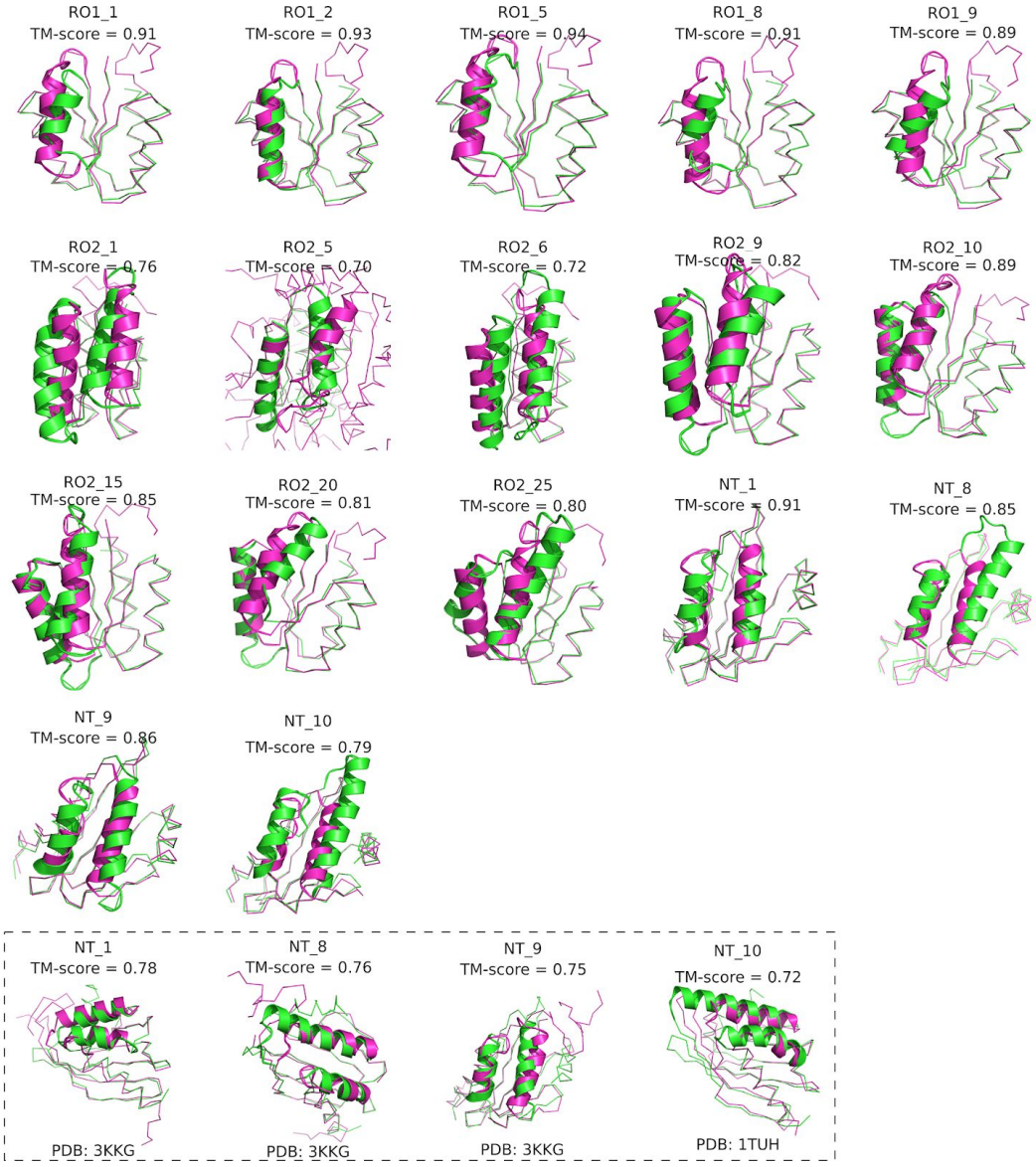

Fig. S9. Models of well-folded designs show considerable geometry differences to their best matches from TM-align. Design models are shown in green and the matched structures are shown in magenta. Except for RO2_5, all Rossmann fold designs matched best to PDB:2KPO which is the *de novo* designed input scaffold PDB:2LV8. All natural proteins in the top 10 TM-align matches to Rossmann fold designs have different topologies from the designed topology. All NTF2 fold designs matched best to the *de novo* designed input scaffold PDB:5TPJ. The last row shows the best natural protein matches to the NTF2 fold designs.

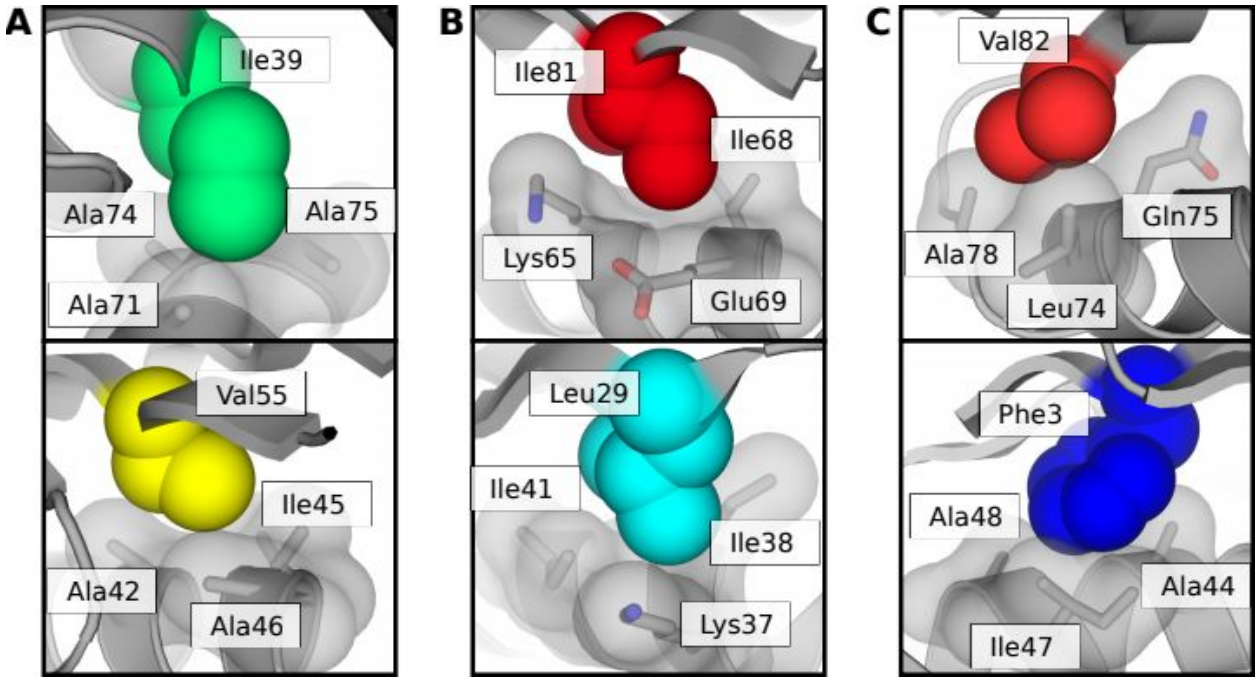

Fig. S10. Residues that form knobs-into-sockets packing. The knob residues shown as colored spheres and the socket residues are shown as grey sticks with transparent surfaces. **A.** RO2_1, **B.** RO2_20 **C.** RO2_25.

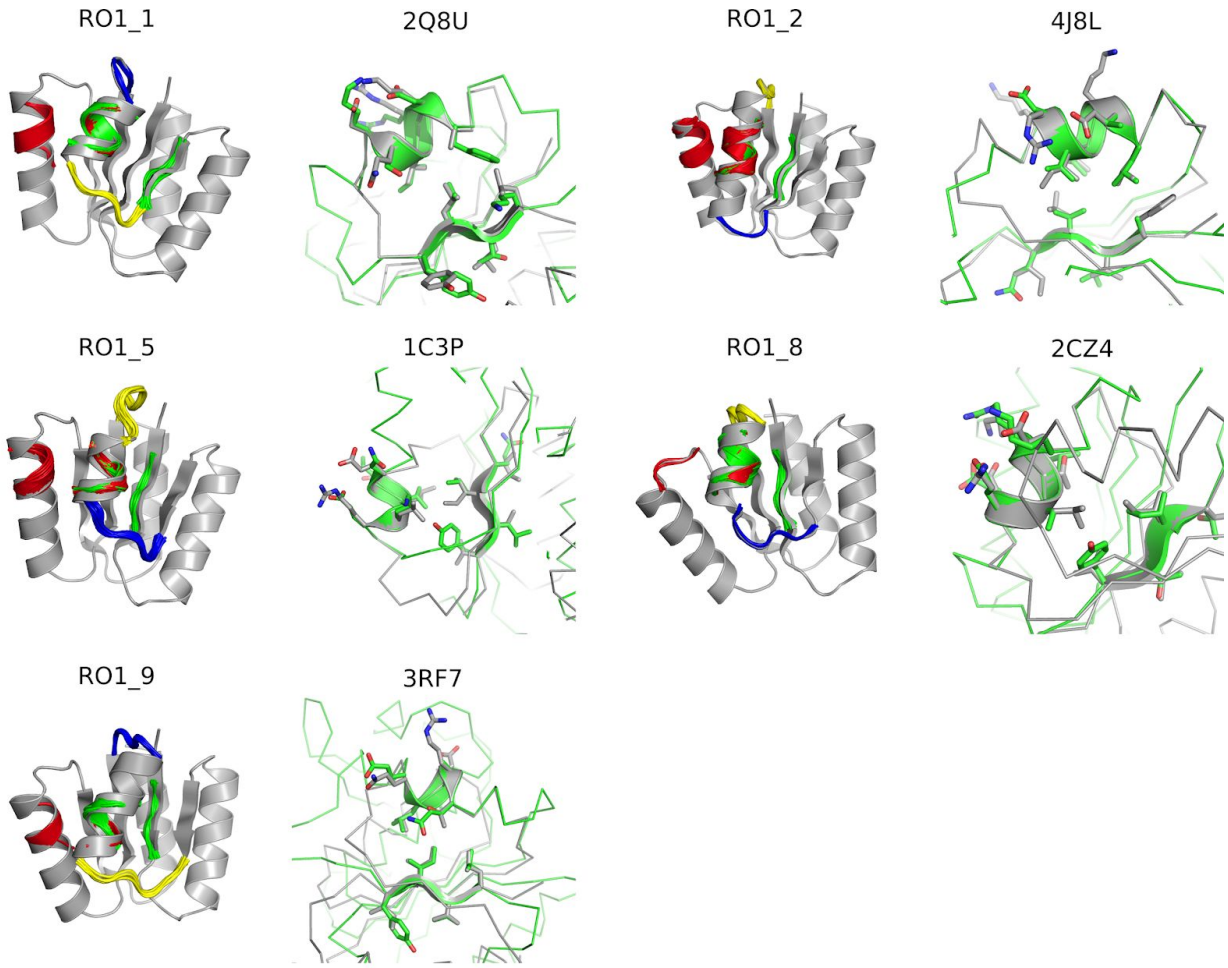

Fig. S11. Identification of tertiary motifs for designed models. For each design, the left panel shows the designed model in grey and the matched tertiary motifs in color. The right panel shows the top match of the green motif. The designs are colored in grey and the source structure of one of the motifs in green. The two structures are superimposed at the motif region. The backbones of the matched region are shown as cartoons and the side chains as sticks. The PDB code of the motif source structures are shown at the top of the right panels.

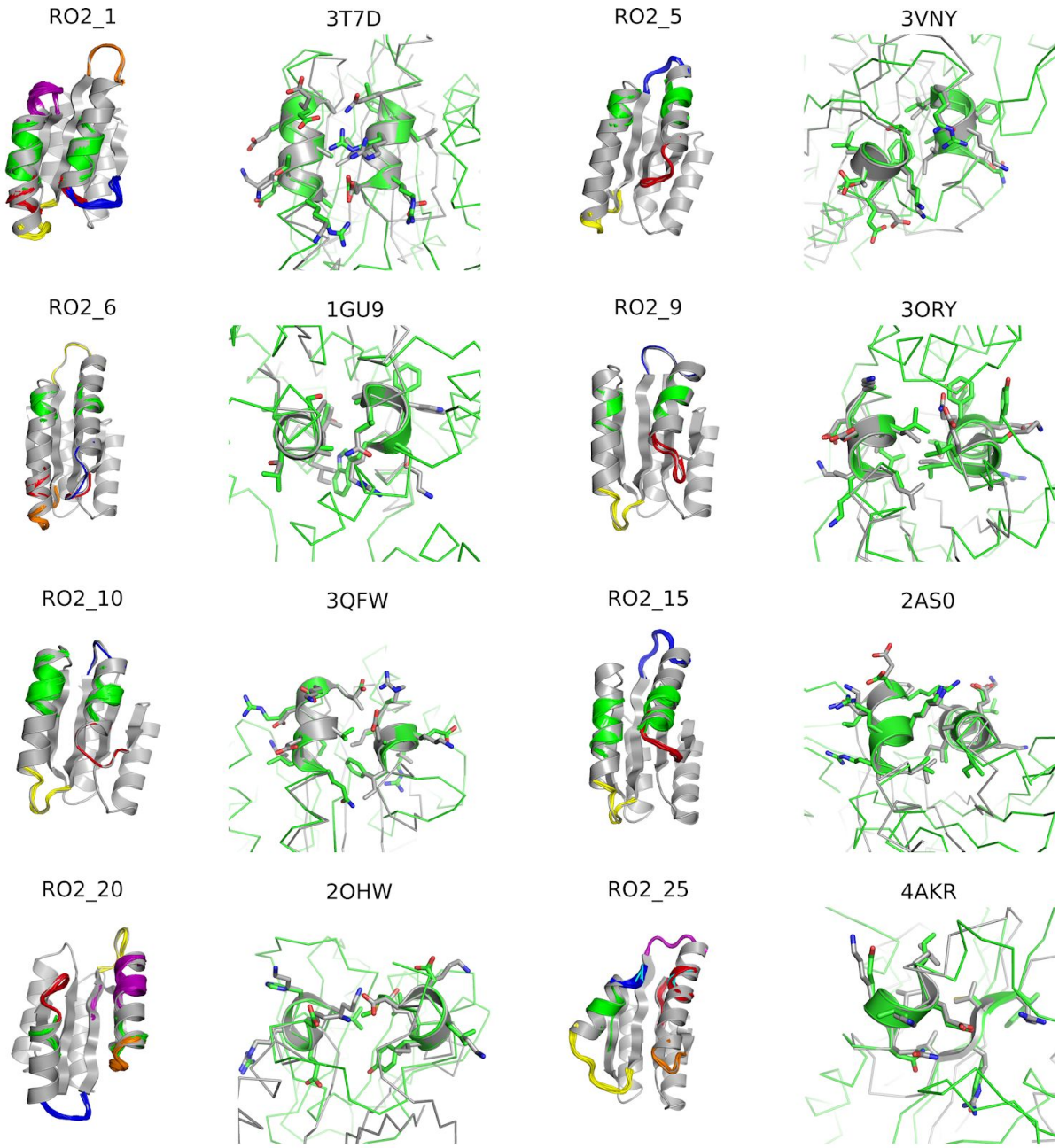

Fig. S11. Identification of tertiary motifs for designed models cont.

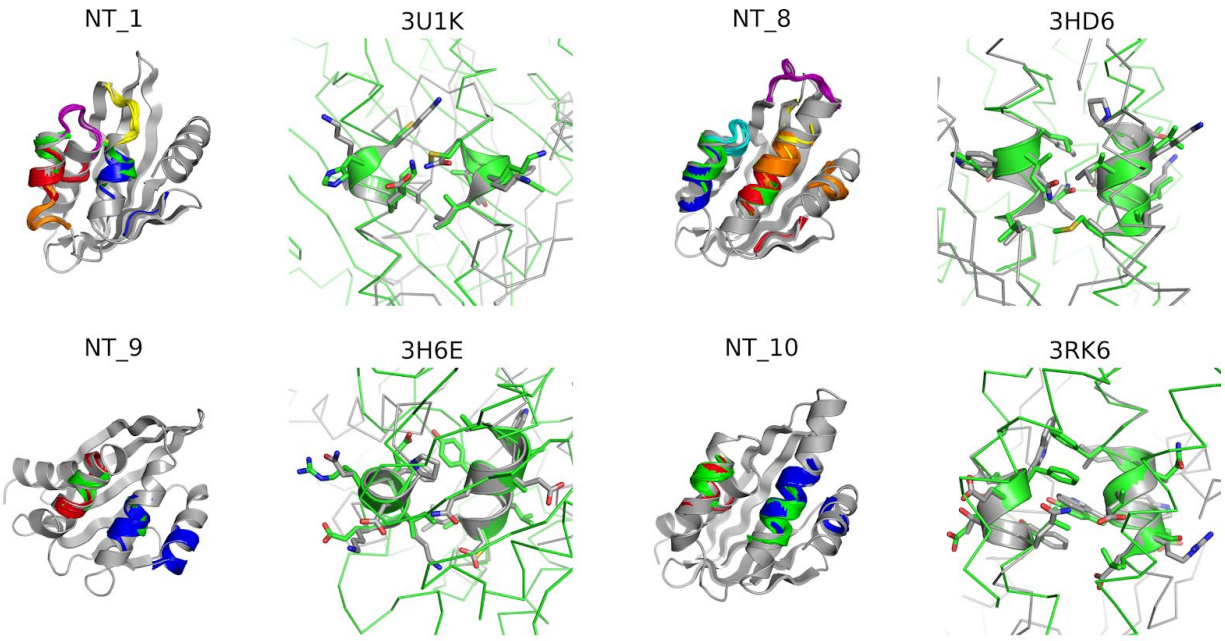

Fig. S11. Identification of tertiary motifs for designed models cont.

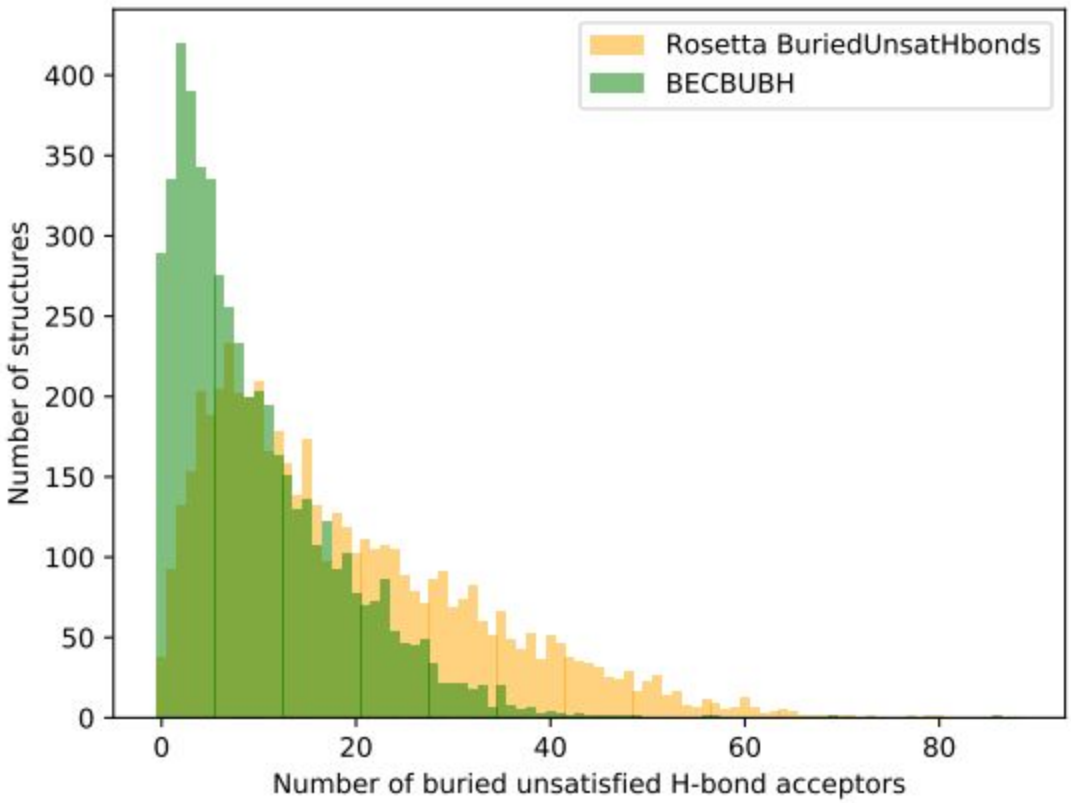

Fig. S12. Number of buried unsatisfied hydrogen bond acceptors found in the top8000 protein structure data set (http://kinemage.biochem.duke.edu/databases/top8000.php). The unsatisfied acceptors found by the Rosetta BuriedUnsatHbonds filter are shown in yellow and the unsatisfied acceptors found by the BECBUBH filter are shown in green.

Table S1. Loop libraries.

Type	Residue number	Number of all loops	Number of non-redundant loops	Degeneracy
Helix-loop-helix	2	45273	224	202
	3	40194	765	52.5
	4	37295	1873	19.9
	5	35118	3656	9.61
Helix-loop-strand	2	6663	224	29.7
	3	15465	788	19.6
	4	24487	1953	12.5
	5	30061	3774	7.97
Strand-loop-helix	2	13263	349	38.0
	3	17819	1183	15.1
	4	21750	2974	7.31
	5	25684	5826	4.41

Table S2. Number of models at each design stage.

Design stage	RO1	RO2	NT
Backbones generated	13421	290836	136683
Sequences designed (iteration 1)	58626	432735	409101
Designs passed filters (iteration 1)	1163	9934	5715
Designs selected for *ab initio* folding	50	n/a	n/a
Sequences designed (iteration 2)		49578	22831
Designs passed filters (iteration 2)		722	98
Designs selected for *ab initio* folding		50	n/a
Designs selected for refinement (iteration 3)			10 (manual)
Sequences designed (iteration 3)			1000
Designs passed filters (iteration 3)			202
Designs selected for *ab initio* folding			50
Designs passed *ab initio* folding	22	25	10
Designs experimentally tested	10	25	10

Table S3. Experimental characterization of designs

Design ID	Soluble	Relative dimer peak size in SEC*	Alpha-beta protein CD spectrum	Well resolved 1D-NMR	15N HSQC with good dispersion
RO1_1	Y	no dimer peak	Y	Y	
RO1_2	Y	no dimer peak	Y	Y	
RO1_3	N				
RO1_4	N				
RO1_5	Y	0.11	Y	Y	
RO1_6	Y				
RO1_7	N				
RO1_8	Y	no dimer peak	Y	Y	
RO1_9	Y	<0.05	Y	Y	
RO1_10	N				
RO2_1	Y	0.06	Y	Y	Y
RO2_2	Y				
RO2_3	N				
RO2_4	N				
RO2_5	Y	no dimer peak	Y	Y	
RO2_6	Y	no dimer peak	Y	Y	
RO2_7	N				
RO2_8	N				
RO2_9	Y	no dimer peak	Y	Y	
RO2_10	Y	no dimer peak	Y	Y	
RO2_11	N				
RO2_12	Y				
RO2_13	Y				
RO2_14	Y				
RO2_15	Y	0.15	Y	Y	
RO2_16	N				
RO2_17	N				
RO2_18	N				
RO2_19	N				
RO2_20	Y	no dimer peak	Y	Y	Y
RO2_21	N				
RO2_22	N				
RO2_23	Y				
RO2_24	Y				

RO2_25	Y	no dimer peak	Y	Y	Y
NT_1	Y	0.09	Y	Y	
NT_2	N				
NT_3	N				
NT_4	N				
NT_5	N				
NT_6	N				
NT_7	N				
NT_8	Y	<0.05	Y	Y	
NT_9	Y	<0.05	Y	Y	
NT_10	Y	<0.05	Y	Y	

Table S4. NMR statistics

	RO2_1	RO2_20	RO2_25
Number of residues	105	100	104
Distance restraints			
Total NOE	1288	1542	2326
intra-residue [i = j]	385	455	577
sequential [| i - j | = 1]	375	426	595
medium range [1 < | i - j | < 5]	203	305	492
long range [| i - j | ≥ 5]	325	356	662
Hydrogen bonds	36	96	36
Dihedral	226	222	230
Violations			
Distance constraints (Å)	0.008±0.001	0.02±0.002	0.014±0.0009
Dihedral angle constraints (°)	1.1±0.7	1.3±0.1	2.2±0.17
Max. distance constraint violation (Å)	0.38	0.37	0.46
Max. dihedral angle restraint violation (°)	14.4	14.2	15.8
Num. Distance violations > 0.3 Å	0.1±0.4	0.6±0.7	1.1±0.7
Num dihedral violations between 5-10°	2.3±2	3.6±1	5.6±2
Num dihedral violations > 10°	0.85±1	0.25±0.5	3.8±1
Validate peaks vs structures (PyRPF)			
Recall	0.985	0.95	0.944
Precision	0.746	0.687	0.793
F-score	0.849	0.798	0.862
DP-score	0.87	0.855	0.9
Structure validation (PSVS)			
Deviations from idealized geometry			
Bond lengths (Å)	0.004	0.004	0.005
Bond angles (°)	0.6	0.7	0.8
Ramachandran plot			
Most favored regions	95.20%	90.90%	86.80%
Additionally allowed regions	4.80%	9.10%	12.40%
Generously allowed regions	0	0.10%	0.60%
Disallowed regions	0	0	0.20%
Average pairwise r.m.s.d. (Å)			
Heavy	1.4	1.4	1.1
Backbone	0.8	0.8	0.6
Structure Quality Factors (raw/Z-scores)			
Procheck G-factor (phi/psi)	0.13/0.83	-0.09/-0.04	-0.17/-0.35
Procheck G-factor (all)	0.01/0.06	-0.15/-0.89	-0.18/-1.06
Verify3D	0.29/-2.73	0.27/-3.05	0.26/-3.21
MolProbity clashscore	8.27/0.11	9.32/-0.07	12.46/-0.61

Table S5. X-ray data reduction and model refinement.

Wavelength	1.116Å
Resolution Range	40.94-1.50 Å (1.53-1.50 Å)
Unit Cell	a=33.50Å , b=51.99Å , c=66.41Å **α**=**β**=***γ***=90°
Space Group	$P2_12_12_1$
Unique Reflections	19203 (895)
Multiplicity	22.7 (12.4)
Completeness	99.9% (92.9%)
<I/σI>	18.5 (1.8)
$CC_{1/2}$	0.999 (0.719)
R_{pim}	0.019 (0.283)
R_{work}	0.1864
R_{free}	0.2104
Total Refined Atoms	1344
Protein Residues	128
Solvent Molecules	81
Refined Ligand Atoms	48
Average B-factor	33.81Å^2
$RMSD_{bonds}$	0.013Å
$RMSD_{angles}$	1.31°
Rama. Plot:	
Favored	98.44%
Allowed	1.56%
Outliers	0.0%
Molprobity Clashscore[d]	3.84
PDB ID	6W90

Data S1. Protein sequences of designs selected for experimental testing.

Design ID	Protein Sequence
RO1_1	KLVVVIDSNDKKLIEEAKKMAEKANLLLLYDVDEDQVRKAAGNARILVLVSNDEQL DKWKEWAQRLELDVRTRKVTSPDEAKRWIKEFSEE
RO1_2	KLFVLILSNDKKLIEEAKKMAEKANLELYVSSSEEDAKRILKELKDRNADSVLVLVS NDEQLDTAKEWAQRLELNVRTRKVTSPDEAKRWIKEFSEE
RO1_3	TLVVVIISNDKKLIEEAKKMAEKANLQLYTDLDPDQAVKLAKKLNADKVLVLVSND EDLDKAKEAAQRAELDVRIRKVTSPDEAKRWIKEFSEE
RO1_4	KLVVIILSNDKKLIEEAQKMAEKANLELYVVDSEELKKLLKKIADENPNTKVLILVSN DEQLDLAKEIAQRLELDVRTRKVTSPDEAKRWIKEFSEE
RO1_5	TLVVIIDSNDKKLIEEAKKMAEKANLELYYERDIEDLLRKLKDADRILILVSNDEQLD KAKEIAQRLEVPVRTRKVTSPDEAKRWIKEFSEE
RO1_6	KLSVIILSNDKKLVEEAKKMAEKANLELYVVTDPDQAEKIIRKLIKEDPTIRILVLVSN DEALDWVKELAQKLEVDLRTRKVTSPDEAKRWIKEFSEE
RO1_7	TLVVIILSNDKKLIEEAKKMAEKANLYLFEVTSDEDWKKAIKTAKEIAKKEQRPLRIL VLVSNDEQLDKAKEIAQRQELDVRTRKVTSPDEAKRWIKEFSEE
RO1_8	TLVVIIDSNDKKLIEEAKKMAEKANLILIESSPDPEKTLRDLNADRVLVLVSNDEQL DTWKEWAQRWELPIRTRKVTSPDEAKRWIKEFSEE
RO1_9	TLLVIILSNDKKLVEEAKKMAEKANLILINSPLSPEQLERTVKSVNADRVLILVSNDE QLDQAKETAQRAELPIRTRKVTSPDEAKRWIKEFSEE
RO1_10	TLVVIIISNDKKLIEEAKKMAEKANLILLVVDNPEEALERAYRLNADKILVLVSNDEQ LDWAKEAAQRWELPVRVRKVTSPDEAKRWIKEFSEE
RO2_1	RLVVLIVSNDKKLIEEARKMAEKANLELITVPGSPEEAIRLAQEIAEKAPGPVKVLV LITGSADPDEKTKAKKAAEEARKWNVRVRTVTSPDEAKRWIKEFSEE
RO2_2	QLYVIISSNDKKLIEEARKMAEKANLNLLTADVDEAYELAKKLIDKAGSAKVLILITG SADPSQKKKIKELAEKARSLNVRIRIVTSPDEAKRWIKEFSEE
RO2_3	TLVVIIVSKDKKLIEEARKMAEKANLLLVVYEPGEDEEAAKEASRRLKESLNNNQP AKVLVLISSSLSPSLAETAAKQLAPDAEVRIRTVTSPDEAKRWIKEFSEE
RO2_4	TLVVFIVSKDKKLIEEARKMAEKANLKLYTAPVSPSIAEKVAKEAKKKNQPAKFLFL VDGTDPTAREIATKLAKYASTVANAEVRIREVTSPDLAKRWIKEFSEE
RO2_5	GLLVIIVSKDKKLIEEARKMAEKANLLLITAPTDPRELETAIKLLQKSNTPIKILILSDG TDPTAEKIAKKLAKEAATKANAEYRIRKVTSPDQAKRWIKEFSEE

RO2_6	GLVVIIVSKDKKLIEEARKMAEKANLYLFTLEPNADPSQLDTLRKWAQEILKRDGP SKLKVLVLSDGTDPTAQKLAKLIAKIVATAANAEVRIRSVTSPDQAKRWIKEFSEE
RO2_7	TLIVVIVSKDKKLIEEARKMAEKANLLLFTGDLTNEQEKTAKEAADRDGSAKILILSD GTDPDARDKATKAAKKLATKLNAEFRIREVTSPDQAKRWIKEFSEE
RO2_8	TLVVIIISDDKKLIEEARKMAEKANLILVTKSEIDDAIREIKKKAKDRPAKILILSDGTN PEAEKIAKKIAEKIAKILNAEVRIRKVTSPDQAKRWIKEFSEE
RO2_9	NLIVFIWSNDKKLIEEARKMAEKANLYLFTLGDNAEKVLQEAVEKVAGDNVKILVLI EDTKDADKLAKKLKEIADKKNWDIRIRKVTSPDEAKRWIKEFSEE
RO2_10	RLIVIILSNDKKLIEEARKMAEKANLELITVRSDEDIEKVLRKAGNAKVLLLIEDTKDA DKLAKKAKEAADKLNVDLRIRKVTSPDEAKRWIKEFSEE
RO2_11	SLFVIIFSNDKKLIEEARKMAEKANLILITVEGSPSAVQEAIKIAVEIARKQNAESIKIL LLVENTKDAEKVKKLAKEAADKLNVDIRIRTVTSPDEAKRWIKEFSEE
RO2_12	SLFVIIYSNDKKLIEEARKMAEKANLNLYTVSGDWREVKKLIEELIKRAKDKNPSEE VKVLLLVKDPRATEAAKKLEKNAPPNVRIRTVTSPDEAKRWIKEFSEE
RO2_13	ELIVLILSNDKKLIEEARKMAEKANLELYTLEGDDEQIKKWIKKLAKTALSRNPSEA KILVLVEDTKDADKKIKIIKKAADEANIEIRIRKVTSPDEAKRWIKEFSEE
RO2_14	QLFVIIVSNDKKLIEEARKMAEKANLELYTADLDTAVKIAKELLKKAEGPAKVLILVS GSASPDQKTKLDKIAKKLRSYNIRLREVTSPDEAKRWIKEFSEE
RO2_15	KLVVLILSNDKKLIEEARKMAEKANLELLTLDGSPEQLKKILKTLLDKAGDRPLKILV LIEDTKDADKWAKAIKEAAKELNIDVRIRKVTSPDEAKRWIKEFSEE
RO2_16	TLIVIIISNDKKLIEEARKMAEKANLNLYTWDDEDKAKKALKDATKYENVKLLFLIEN TKDAEKIEKKIKDTAKKLNLDVRVRLVTSPDEAKRWIKEFSEE
RO2_17	TLIVVIWSNDKKLIEEARKMAEKANLLLLTVTSDEDLKKAAKIAQSAPGEVKVLLLV EDTKDADKIADKAKKIFKKANVDIRIRKVTSPDEAKRWIKEFSEE
RO2_18	TLVVLIWSNDKKLIEEARKMAEKANLYLITVGDDKALEKAIRTAEKIAKDNNADSFK ILILIEDTKDADKISKKAKDIASKLNIEIRVRKVTSPDEAKRWIKEFSEE
RO2_19	TLIVLIISNDKKLIEEARKMAEKANLLLYTLEPNQDPSIEKEIKTIQKRADPRDLKILVL IENTKDAEKIATEIKRKAEKNNLNVRIRLVTSPDEAKRWIKEFSEE
RO2_20	GLLVLIWSNDKKLIEEARKMAEKANLYLLTLETDDKKIEDILKSLGPPVKILVLLEDT KDADKVKKEIEKKARKKNLPVRIRKVTSPDEAKRWIKEFSEE
RO2_21	TLIVIIISNDKKLIEEARKMAEKANLVLITDEGSPSAEEKLKKTITDAKRKDPTDPVKI LVLIEDTKDADKIAEEIKRKADKANWDVRIRKVTSPDEAKRWIKEFSEE
RO2_22	TLVVLIFSNDKKLIEEARKMAEKANLELYTRSELDPNIVTKLRDNAENAKLLVLIEDT KDADKLAEKIKKALDKNNIDVRIRKVTSPDEAKRWIKEFSEE

RO2_23	SLVVFIWSNDKKLIEEARKMAEKANLELITVSSIDQAIKLAREIAKKQKRPAKFLILV SGSLDPSQKKKVDEIAKEARKDNIRVRTVTSPDEAKRWIKEFSEE
RO2_24	KLLVVILSNDKKLIEEARKMAEKANLELITVTSLEEAKKAAEKALKEANGNAKVLVLI TGSADPTQKKKATEWAKKAKDYNIRVRTVTSPDEAKRWIKEFSEE
RO2_25	TLFVLILSNDKKLIEEARKMAEKANLILITVGDEEELKKAIKKADDIAKKQNSSEAKIL ILLEKPVSPEYEKKLQKYADAEVRVRTVTSPDEAKRWIKEFSEE
NT_1	SREEIRKVVETFLRAANSQDKKKLEEAAKNILSPDVRLEVGNYTWTSIEQMLKFY QLSEIDRVEIRKVQVDGNHVRVEIEVERNGKKWTWEVEVEVRNGLIKRIRNQVDP EYKKDVQNIWNNT
NT_2	SREEIRKVVEEFIRAQEDPDKLEKVASKALSPDVRVEIGNFTLEDKKQVIKWQKAF YKVLQEKAGKDASFRYEIRKVQVDGNHVRVEVEVETNGKKWTYEIELEVRNGKI KRIRLQVDPEYKEIVQLAWNRT
NT_3	SREEIRKVVETWVRLFNSGDPRDRKKYEKAQKELLSPDVRTEIGNYTIEPGTLER FVQAYWKVLDELWPNVPIRVEIRKVQVDGNHVRIEVEVEINGKKYTFEIEVEVRN GKIKRIRIQRDPEMKELIQIAWNRT
NT_4	SREEIRKVVETYVRISLSSSEETKKILRDLLSPDARLEFGNYTIESGDIWKFMQLF WKYYAGDAPLRLEIRKVQVDGNHVRIEVEVETKGKKWTYEIEVEVRNGKIKRVRT QVDPEYKKALQYAWNAT
NT_5	SREEIRKIVELFVKAWDNPDAREKFEKNKDKVLSPDVRLEIGNFTLENKDKLESFY RVLIKLWQEKAGPNVRIEIRKVQVDGNHVRVEVEVETNGKKWTYEIEVEVRNGTI KRIRTQYDPEYKKDIQQAWNLS
NT_6	SREEIRKIVETIVRANRDTSLFEKLAKELNLFSPDTRIEIGNYTFEGDAIKVIKAYIEA NLQFAKKVSKDAPVRIEIRKVQVDGNHVRVEVEIELAGKKFTTEIEVEVRNGVVKR IRIQVDPEFKKLVQYAWNKT
NT_7	SREEIRKVVEIFIRLQSLDPSQLEKALKDLNILSPDVRLEVGNITLNSADKLIRFLALI TEILIRLWTGKPAPLRVEIRKVQVDGNHVRVEIEQEINGRKWTYEIEFEVRNGVIK RIRVQLDPSTKEAVQRAWNLT
NT_8	SREEIRKVVETFVRAKQDPREFTKALSLLSPDVRMEIGNYTLTSIRDIKRFFEALVE IWKRKNLTDWRYEIRKVQVDGNHVRIEVETQTDGKKWTWEIEIEVRNGKIKRIRE QYDPEYKKDVQLAWNLT
NT_9	SREEIRKVVEEYIRLLYTDPDQFKKAARDKLLSPDVRIEIGNYTFDSRNLDRFLDA MQEWASRYDRVEIRKVQVDGNHVRVEIELESNGKKWTFEIEVEVRNGKIKRIRQ QVDPEYKKVVQNLWNNT
NT_10	SREEIRKVVETWIRLFYSSDPNDWETFQKAKKDLLSPDVRVEIGNYTLNSEQVDR WWEAWVKIIQKELEEKNEPLRTEIRKVQVDGNHVRVEIEQEKNGKKWTFEVEVE VRNGKIKRIRQQVDPEYKKEVQAAWNNT

Data S2. DNA sequences of designs selected for experimental testing

Design ID	DNA Sequence
RO1_1	AAACTGGTGGTGGTGATTGATAGCAACGATAAAAAACTGATTGAAGAAGCGAAAAAAATGGCGGAAAAAGC GAACCTGCTGCTGCTGTATGATGTGGATGAAGATCAGGTGCGTAAAGCGGCGGGCAACGCGCGTATTCTGGT GCTGGTGAGCAACGATGAACAGCTGGATAAATGGAAAGAATGGGCGCAGCGTCTGGAACTGGATGTGCGTA CCCGTAAAGTGACCAGCCCGGATGAAGCGAAACGTTGGATTAAAGAATTTAGCGAAGAATAATAAGGCAGCT AAGGCAGCTAAGGC
RO1_2	AAACTGTTTGTGCTGATTCTGAGCAACGATAAAAAACTGATTGAAGAAGCGAAAAAAATGGCGGAAAAAGCG AACCTGGAACTGTATGTGAGCAGCAGCGAAGAAGATGCGAAACGTATTCTGAAAGAACTGAAAGATCGTAAC GCGGATAGCGTGCTGGTGCTGGTGAGCAACGATGAACAGCTGGATACCGCGAAAGAATGGGCGCAGCGTCT GGAACTGAACGTGCGTACCCGTAAAGTGACCAGCCCGGATGAAGCGAAACGTTGGATTAAAGAATTTAGCGA AGAATAATAAGGC
RO1_3	ACCCTGGTGGTGGTGATTATTAGCAACGATAAAAAACTGATTGAAGAAGCGAAAAAAATGGCGGAAAAAGCG AACCTGCAGCTGTATACCGATCTGGATCCGGATCAGGCGGTGAAACTGGCGAAAAAACTGAACGCGGATAAA GTGCTGGTGCTGGTGAGCAACGATGAAGATCTGGATAAAGCGAAAGAAGCGGCGCAGCGTGCGGAACTGGA TGTGCGTATTCGTAAAGTGACCAGCCCGGATGAAGCGAAACGTTGGATTAAAGAATTTAGCGAAGAATAATA AGGCAGCTAAGGC
RO1_4	AAACTGGTGGTGATTATTCTGAGCAACGATAAAAAACTGATTGAAGAAGCGCAGAAAATGGCGGAAAAAGCG AACCTGGAACTGTATGTGGTGGATAGCGAAGAACTGAAAAAACTGCTGAAAAAAATTGCGGATGAAAACCCG AACACCAAAGTGCTGATTCTGGTGAGCAACGATGAACAGCTGGATCTGGCGAAAGAAATTGCGCAGCGTCTG GAACTGGATGTGCGTACCCGTAAAGTGACCAGCCCGGATGAAGCGAAACGTTGGATTAAAGAATTTAGCGAA GAATAATAAGGC
RO1_5	ACCCTGGTGGTGATTATTGATAGCAACGATAAAAAACTGATTGAAGAAGCGAAAAAAATGGCGGAAAAAGCG AACCTGGAACTGTATTATGAACGTGATATTGAAGATCTGCTGCGTAAACTGAAAGATGCGGATCGTATTCTGA TTCTGGTGAGCAACGATGAACAGCTGGATAAAGCGAAAGAAATTGCGCAGCGTCTGGAAGTGCCGGTGCGTA CCCGTAAAGTGACCAGCCCGGATGAAGCGAAACGTTGGATTAAAGAATTTAGCGAAGAATAATAAGGCAGCT AAGGCAGCTAA
RO1_6	AAACTGAGCGTGATTATTCTGAGCAACGATAAAAAACTGGTGGAAGAAGCGAAAAAAATGGCGGAAAAAGC GAACCTGGAACTGTATGTGGTGACCGATCCGGATCAGGCGGAAAAAATTATTCGTAAACTGATTAAAGAAGAT CCGACCATTCGTATTCTGGTGCTGGTGAGCAACGATGAAGCGCTGGATTGGGTGAAAGAACTGGCGCAGAAA CTGGAAGTGGATCTGCGTACCCGTAAAGTGACCAGCCCGGATGAAGCGAAACGTTGGATTAAAGAATTTAGC GAAGAATAATAA
RO1_7	ACCCTGGTGGTGATTATTCTGAGCAACGATAAAAAACTGATTGAAGAAGCGAAAAAAATGGCGGAAAAAGCG AACCTGTATCTGTTTGAAGTGACCAGCGATGAAGATTGGAAAAAAGCGATTAAAACCGCGAAAGAAATTGCG AAAAAAGAACAGCGTCCGCTGCGTATTCTGGTGCTGGTGAGCAACGATGAACAGCTGGATAAAGCGAAAGAA ATTGCGCAGCGTCAGGAACTGGATGTGCGTACCCGTAAAGTGACCAGCCCGGATGAAGCGAAACGTTGGATT AAAGAATTTAGCGAAGAATAA
RO1_8	ACCCTGGTGGTGATTATTGATAGCAACGATAAAAAACTGATTGAAGAAGCGAAAAAAATGGCGGAAAAAGCG AACCTGATTCTGATTGAAAGCAGCCCGGATCCGGAAAAAACCCTGCGTGATCTGAACGCGGATCGTGTGCTGG TGCTGGTGAGCAACGATGAACAGCTGGATACCTGGAAAGAATGGGCGCAGCGTTGGGAACTGCCGATTCGTA

	CCCGTAAAGTGACCAGCCCGGATGAAGCGAAACGTTGGATTAAAGAATTTAGCGAAGAATAATAAGGCAGCTAAGGCAGCTAA
RO1_9	ACCCTGCTGGTGATTATTCTGAGCAACGATAAAAAACTGGTGGAAGAAGCGAAAAAAATGGCGGAAAAAGCGAACCTGATTCTGATTAACAGCCCGCTGAGCCCGGAACAGCTGGAACGTACCGTGAAAAGCGTGAACGCGGATCGTGTGCTGATTCTGGTGAGCAACGATGAACAGCTGGATCAGGCGAAAGAAACCGCGCAGCGTGCGGAACTGCCGATTCGTACCCGTAAAGTGACCAGCCCGGATGAAGCGAAACGTTGGATTAAAGAATTTAGCGAAGAATAATAAGGCAGCTAA
RO1_10	ACCCTGGTGGTGATTATTATTAGCAACGATAAAAAACTGATTGAAGAAGCGAAAAAAATGGCGGAAAAAGCGAACCTGATTCTGCTGGTGGTGGATAACCCGGAAGAAGCGCTGGAACGTGCGTATCGTCTGAACGCGGATAAAATTCTGGTGCTGGTGAGCAACGATGAACAGCTGGATTGGGCGAAAGAAGCGGCGCAGCGTTGGGAACTGCCGGTGCGTGTGCGTAAAGTGACCAGCCCGGATGAAGCGAAACGTTGGATTAAAGAATTTAGCGAAGAATAATAAGGCAGCTAAGGC
RO2_1	CGCCTTGTTGTATTGATCGTAAGTAATGACAAGAAGTTGATCGAAGAGGCCCGCAAGATGGCTGAGAAGGCTAATTTGGAGTTGATCACGGTTCCAGGTAGTCCTGAGGAAGCCATCCGCTTGGCTCAAGAGATCGCCGAGAAGGCTCCTGGGCCCGTTAAGGTATTGGTCTTAATCACAGGTTCAGCCGACCCCGACGAGAAGACGAAGGCCAAGAAGGCAGCAGAGGAAGCTCGCAAGTGGAATGTCCGCGTTCGCACGGTTACATCTCCTGACGAGGCAAAGCGCTGGATCAAGGAGTTCTCAGAGGAGTGA
RO2_2	CAGCTGTATGTGATTATTTCCAGTAACGATAAGAAACTGATTGAAGAGGCGCGTAAAATGGCGGAAAAGGCAAACCTGAACCTGCTTACAGCCGATGTGGATGAAGCGTATGAACTGGCGAAGAAATTGATTGATAAAGCAGGGAGCGCGAAAGTACTTATTCTGATTACCGGCAGTGCGGATCCCTCTCAGAAGAAGAAAATTAAAGAACTCGCGGAAAAGGCACGTAGCTTAAACGTACGTATTCGTATTGTTACCAGCCCGGATGAAGCGAAACGTTGGATTAAAGAATTTTCGGAAGAATAA
RO2_3	ACACTCGTTGTCATCATCGTATCGAAGGACAAGAAGCTTATCGAAGAGGCCCGCAAGATGGCTGAGAAGGCTAATTTGCTCTTGGTCGTTTACGAGCCAGGTGAGGACGAAGAGGCAGCCAAAGAGGCCAGTCGCCGCTTAAAGGAGTCTCTCAATAATAATCAACCTGCAAAGGTCTTGGTTCTCATCTCAAGTTCCCTCTCACCTAGTTTAGCCGAGACGGCAGCCAAGCAATTGGCCCCAGACGCTGAGGTACGCATCCGCACGGTAACATCTCCAGACGAGGCAAAGCGCTGGATCAAGGAGTTCTCTGAGGAGTGA
RO2_4	ACTTTAGTCGTTTTCATCGTTAGTAAGGACAAGAAGCTCATCGAGGAAGCCCGCAAGATGGCCGAGAAGGCCAATCTTAAGCTCTACACAGCTCCAGTTTCCCCCTCTATCGCCGAGAAGGTCGCTAAAGAGGCAAAGAAGAAGAATCAACCAGCAAAGTTCCTCTTCCTCGTTGACGGTACGGACCCCACAGCACGCGAGATCGCCACAAAGTTAGCCAAGTACGCATCAACTGTCGCCAATGCCGAGGTCCGCATCCGCGAGGTTACTTCTCCTGACCTTGCAAAGCGCTGGATCAAGGAGTTCTCAGAGGAGTGA
RO2_5	GGTCTCCTCGTAATCATCGTTAGCAAGGACAAGAAGTTAATTGAAGAAGCTCGCAAGATGGCCGAGAAGGCAAATTTATTGTTAATCACAGCACCTACGGACCCACGCGAGTTGGAGACTGCAATCAAGTTACTTCAAAAGTCAAATACGCCAATCAAGATCTTAATCTTATCAGACGGAACGGACCCCACGGCTGAGAAGATCGCAAAGAAGTTGGCCAAGGAAGCAGCAACGAAGGCCAATGCCGAGTACCGCATCCGCAAGGTTACTTCACCCGACCAAGCAAAGCGCTGGATCAAGGAGTTCTCTGAGGAGTGA
RO2_6	GGGCTCGTAGTCATCATCGTTTCTAAGGACAAGAAGTTAATCGAAGAGGCCCGCAAGATGGCCGAGAAGGCCAATTTATACTTATTCACGTTAGAGCCAAATGCCGACCCAAGTCAATTGGACACGCTCCGCAAGTGGGCCCAAGAGATCCTTAAGCGCGACGGGCCCTCAAAGCTCAAGGTATTGGTTCTCTCGGACGGTACGGACCCCACAGCACAAAAGTTGGCCAAGCTTATCGCAAAGATCGTAGCAACGGCAGCCAATGCCGAGGTTCGCATCCGCTCCGTAACTTCACCTGACCAAGCCAAGCGCTGGATCAAGGAGTTCTCCGAGGAGTGA

RO2_7	ACTCTCATCGTCGTTATCGTATCTAAGGACAAGAAGTTAATCGAGGAAGCCCGCAAGATGGCCGAGAAGGCCA ATTTACTCTTATTCACTGGAGACCTCACGAATGAGCAAGAGAAGACAGCAAAAGAGGCTGCCGACCGCGACG GATCAGCTAAGATCCTTATCCTTAGTGACGGTACGGACCCTGACGCTCGCGACAAGGCTACGAAGGCCGCCAA GAAGCTCGCAACAAAGCTTAATGCTGAGTTCCGCATCCGCGAGGTAACGTCACCTGACCAAGCCAAGCGCTGG ATCAAGGAGTTCAGTGAGGAGTGA
RO2_8	ACATTGGTTGTTATCATCATCTCAGACGACAAGAAGTTGATCGAGGAAGCACGCAAGATGGCTGAGAAGGCA AATTTAATCTTGGTTACGAAGAGTGAGATCGACGACGCAATCCGCGAGATCAAGAAGAAGGCCAAGGACCGC CCTGCCAAGATCTTAATCTTAAGTGACGGGACGAATCCAGAGGCAGAGAAGATCGCTAAGAAGATCGCAGAG AAGATCGCCAAGATCCTCAATGCCGAGGTACGCATCCGCAAGGTAACGAGTCCTGACCAAGCAAAGCGCTGG ATCAAGGAGTTCAGTGAGGAGTGA
RO2_9	AATTTGATCGTTTTCATCTGGTCCAATGACAAGAAGCTTATCGAAGAGGCCCGCAAGATGGCAGAGAAGGCAA ATTTGTACCTCTTCACGTTGGGAGACAATGCTGAGAAGGTTTTACAAGAGGCCGTTGAGAAGGTTGCCGGTGA CAATGTAAAGATCTTGGTTTTGATCGAGGACACGAAGGACGCTGACAAGCTTGCAAAGAAGTTAAAGGAGAT CGCAGACAAGAAGAATTGGGACATCCGCATCCGCAAGGTAACTTCGCCAGACGAGGCTAAGCGCTGGATCAA GGAGTTCTCTGAGGAGTGA
RO2_10	CGCTTGATCGTAATCATTCTGTCCAATGACAAGAAGCTTATCGAAGAGGCCCGCAAGATGGCCGAGAAGGCAA ATCTTGAGCTTATCACAGTTCGCAGTGACGAGGACATCGAGAAGGTATTACGCAAGGCCGGGAATGCAAAGG TCCTTTTGCTTATCGAGGACACGAAGGACGCCGACAAGTTGGCCAAGAAGGCCAAGGAAGCCGCCGACAAGT TGAATGTAGACCTTCGCATCCGCAAGGTAACGTCTCCTGACGAGGCTAAGCGCTGGATCAAGGAGTTCAGTGA GGAGTGATAA
RO2_11	TCGTTGTTCGTCATCATCTTCTCAAATGACAAGAAGCTTATCGAGGAAGCCCGCAAGATGGCAGAGAAGGCCA ATTTGATCTTGATCACAGTCGAGGGTTCTCCTTCTGCAGTCCAAGAGGCAATCAAGATCGCCGTTGAGATCGCA CGCAAGCAAAATGCAGAGTCGATCAAGATCTTGCTTTTAGTCGAGAATACAAAGGACGCAGAGAAGGTTAAG AAGCTCGCCAAAGAGGCCGCCGACAAGTTAAATGTTGACATCCGCATCCGCACTGTTACGTCTCCAGACGAGG CTAAGCGCTGGATCAAGGAGTTCTCCGAGGAGTGA
RO2_12	AGTCTTTTCGTTATCATCTACTCGAATGACAAGAAGCTCATCGAGGAAGCACGCAAGATGGCAGAGAAGGCTA ATCTTAATTTATACACGGTTTCGGGAGACTGGCGCGAGGTTAAGAAGCTTATCGAGGAGTTGATCAAGCGCGC CAAGGACAAGAATCCATCTGAGGAAGTTAAGGTCTTACTTTTAGTCAAGGACCCTCGCGCCACTGAGGCTGCC AAGAAGTTAGAGAAGAATGCACCCCCAAATGTTCGCATCCGCACTGTTACGTCTCCCGACGAGGCCAAGCGCT GGATCAAGGAGTTCTCAGAGGAGTGA
RO2_13	GAGTTGATCGTTTTGATCCTTTCGAATGACAAGAAGCTCATCGAGGAAGCACGCAAGATGGCAGAGAAGGCC AATCTCGAATTGTACACGTTGGAAGGTGACGACGAGCAAATCAAGAAGTGGATCAAGAAGCTCGCCAAGACT GCCTTGTCTCGCAATCCCAGTGAGGCAAAGATCTTAGTCCTTGTTGAGGACACTAAGGACGCAGACAAGAAGA TCAAGATCATCAAGAAGGCCGCCGACGAGGCAAATATCGAGATCCGCATCCGCAAGGTTACATCACCCGACG AGGCAAAGCGCTGGATCAAGGAGTTCTCAGAGGAGTGA
RO2_14	CAACTCTTCGTCATCATCGTATCAAATGACAAGAAGCTTATTGAAGAGGCACGCAAGATGGCAGAGAAGGCCA ATCTCGAACTTTACACGGCAGACTTAGACACTGCAGTAAAGATCGCCAAGGAGTTGTTGAAGAAGGCCGAGG GGCCAGCTAAGGTCCTCATCTTAGTCTCAGGGTCAGCATCGCCAGACCAAAAGACAAAGTTAGACAAGATCGC CAAGAAGCTTCGCTCGTACAATATCCGCTTACGCGAGGTTACGTCTCCAGACGAGGCAAAGCGCTGGATCAAG GAGTTCAGCGAGGAGTGA
RO2_15	AAGCTGGTCGTCTTGATCTTGAGCAATGACAAGAAGTTGATTGAAGAGGCCCGCAAGATGGCCGAGAAGGCA AATTTGGAGTTGCTTACGTTAGACGGTTCACCTGAGCAACTCAAGAAGATCCTTAAGACGCTTTTAGACAAGG

	CCGGAGACCGCCCATTGAAGATCTTGGTCTTGATCGAGGACACGAAGGACGCCGACAAGTGGGCCAAGGCAA TCAAAGAGGCCGCCAAGGAGCTCAATATCGACGTCCGCATCCGCAAGGTCACATCCCCTGACGAGGCCAAGC GCTGGATCAAGGAGTTCTCGGAAGAGTGA
RO2_16	ACACTTATCGTCATCATCATCTCGAATGACAAGAAGCTCATCGAGGAAGCCCGCAAGATGGCCGAGAAGGCCA ATTTAAATCTCTACACGTGGGACGACGAGGACAAGGCTAAGAAGGCATTAAAGGACGCAACTAAGTACGAGA ATGTTAAGTTATTATTCCTCATCGAGAATACTAAGGACGCCGAGAAGATCGAGAAGAAGATCAAGGACACGG CAAAGAAGCTCAATTTAGACGTCCGCGTTCGCTTGGTTACGTCGCCAGACGAGGCCAAGCGCTGGATCAAGG AGTTCTCAGAGGAGTGA
RO2_17	ACATTAATCGTCGTAATCTGGTCCAATGACAAGAAGTTAATCGAAGAGGCACGCAAGATGGCTGAGAAGGCA AATCTCCTCTTATTGACAGTTACTTCCGACGAGGACTTGAAGAAGGCAGCAAAGATCGCACAAAGTGCCCCAG GAGAGGTAAAGGTCCTTCTCCTTGTTGAGGACACAAAGGACGCTGACAAGATCGCCGACAAGGCCAAGAAGA TCTTCAAGAAGGCCAATGTAGACATCCGCATCCGCAAGGTTACGTCGCCTGACGAGGCCAAGCGCTGGATCAA GGAGTTCTCCGAGGAGTGA
RO2_18	ACACTTGTAGTCTTAATCTGGTCGAATGACAAGAAGCTTATCGAAGAGGCACGCAAGATGGCCGAGAAGGCC AATCTCTACCTTATCACGGTCGGTGACGACAAGGCCTTGGAGAAGGCTATCCGCACGGCAGAGAAGATCGCA AAGGACAATAATGCCGACTCTTTCAAGATCTTAATCCTTATCGAGGACACAAAGGACGCCGACAAGATCAGTA AGAAGGCAAAGGACATCGCCAGCAAGCTCAATATCGAGATCCGCGTTCGCAAGGTAACATCTCCTGACGAGG CTAAGCGCTGGATCAAGGAGTTCTCTGAGGAGTGA
RO2_19	ACTTTAATCGTTTTGATCATCTCGAATGACAAGAAGTTGATCGAGGAAGCCCGCAAGATGGCCGAGAAGGCTA ATTTATTACTTTACACTCTTGAGCCTAATCAAGACCCATCCATCGAGAAGGAGATCAAGACGATCCAAAAGCGC GCTGACCCACGCGACTTAAAGATCCTTGTTCTTATCGAGAATACTAAGGACGCAGAGAAGATCGCCACGGAGA TCAAGCGCAAGGCAGAGAAGAATAATTTAAATGTACGCATCCGCCTTGTCACGTCGCCCGACGAGGCCAAGC GCTGGATCAAGGAGTTCAGTGAGGAGTGA
RO2_20	GGATTATTGGTCCTCATTTGGTCGAATGACAAGAAGCTCATCGAGGAAGCTCGCAAGATGGCTGAGAAGGCC AATCTCTACCTCTTGACGCTCGAAACTGACGACAAGAAGATCGAGGACATCTTAAAGTCGCTCGGGCCGCCCG TTAAGATCCTCGTTCTCTTAGAGGACACAAAGGACGCCGACAAGGTCAAGAAGGAGATCGAGAAGAAGGCCC GCAAGAAGAATTTACCCGTACGCATCCGCAAGGTAACTTCGCCAGACGAGGCAAAGCGCTGGATCAAGGAGT TCAGTGAGGAGTGA
RO2_21	ACTTTGATTGTCATCATCATCAGTAACGACAAGAAGTTGATCGAGGAAGCTCGCAAGATGGCTGAGAAGGCCA ATCTCGTCTTGATCACTGACGAGGGAAGTCCCAGTGCAGAGGAGAAGCTCAAGAAGACAATCACGGACGCCA AGCGCAAGGACCCAACGGACCCAGTAAAGATCTTAGTATTAATCGAGGACACTAAGGACGCCGACAAGATCG CCGAGGAGATCAAGCGCAAGGCTGACAAGGCAAATTGGGACGTCCGCATCCGCAAGGTAACATCCCCAGACG AGGCAAAGCGCTGGATCAAGGAGTTCTCCGAGGAGTGA
RO2_22	ACTTTGGTTGTTTTGATCTTCTCGAATGACAAGAAGTTGATCGAAGAGGCACGCAAGATGGCAGAGAAGGCA AATCTCGAACTTTACACTCGCAGTGAGTTGGACCCAAATATCGTAACAAAGCTCCGCGACAATGCAGAGAATG CCAAGCTTCTTGTATTGATCGAGGACACGAAGGACGCAGACAAGCTCGCCGAGAAGATCAAGAAGGCCCTCG ACAAGAATAATATCGACGTACGCATCCGCAAGGTAACGTCGCCTGACGAGGCCAAGCGCTGGATCAAGGAGT TCTCTGAGGAGTGA
RO2_23	TCATTAGTTGTCTTCATCTGGTCCAATGACAAGAAGTTGATCGAGGAAGCTCGCAAGATGGCAGAGAAGGCTA ATTTGGAGTTGATCACGGTCAGTTCAATCGACCAAGCAATCAAGTTGGCCCGCGAGATCGCAAAGAAGCAAAA GCGCCCTGCCAAGTTCTTGATCTTGGTCTCAGGGAGTTTAGACCCCTCTCAAAAGAAGAAGGTTGACGAGATC

	GCTAAAGAGGCCCGCAAGGACAATATCCGCGTTCGCACAGTCACTTCGCCTGACGAGGCCAAGCGCTGGATC AAGGAGTTCAGTGAGGAGTGA
RO2_24	AAGTTGCTCGTTGTTATCCTTAGTAATGACAAGAAGTTGATCGAGGAAGCACGCAAGATGGCAGAGAAGGCA AATTTAGAGTTAATCACGGTTACATCGCTTGAAGAGGCCAAGAAGGCCGCAGAGAAGGCCTTGAAAGAGGCA AATGGTAATGCCAAGGTACTCGTTTTAATCACTGGGTCCGCCGACCCAACGCAAAAGAAGAAGGCAACTGAGT GGGCAAAGAAGGCTAAGGACTACAATATCCGCGTACGCACAGTAACATCTCCAGACGAGGCCAAGCGCTGGA TCAAGGAGTTCAGCGAGGAGTGA
RO2_25	ACGCTTTTCGTACTCATCTTATCAAATGACAAGAAGCTTATCGAGGAAGCCCGCAAGATGGCAGAGAAGGCCA ATTTGATCCTCATCACGGTCGGGGACGAAGAGGAGTTAAAGAAGGCCATCAAGAAGGCCGACGACATCGCTA AGAAGCAAAATTCGTCAGAGGCCAAGATCCTCATCTTGCTTGAGAAGCCAGTCTCGCCTGAGTACGAGAAGAA GTTACAAAAGTACGCAGACGCAGAGGTTCGCGTTCGCACAGTTACGTCACCAGACGAGGCCAAGCGCTGGAT CAAGGAGTTCTCTGAGGAGTGA
NT_1	TCGCGCGAGGAGATCCGTAAAGTAGTCGAAACCTTTCTGCGTGCTGCGAATAGCCAGGACAAAAAAAAACTC GAAGAGGCGGCGAAAAATATTCTGTCACCTGATGTTCGTCTGGAAGTCGGCAACTATACCTGGACCAGCATTG AACAAATGCTTAAGTTTTATCAACTGTCTGAGATTGATCGCGTCGAAATTCGCAAAGTGCAGGTCGATGGCAA CCACGTGCGTGTGGAAATTGAAGTAGAACGTAATGGCAAAAAGTGGACCTGGGAAGTTGAGGTGGAAGTAC GTAATGGTTTGATTAAACGCATTCGTAATCAGGTCGATCCGGAATATAAAAAAGATGTGCAAAATATCTGGAA TAATACCTAA
NT_2	AGCCGCGAAGAAATCCGTAAAGTAGTGGAAGAATTTATCCGTGCGCAAGAAGATCCCGACAAACTCGAGAAA GTAGCGTCAAAGGCGCTGTCCCCGGACGTCCGCGTCGAAATTGGCAATTTCACATTGGAAGATAAGAAGCAG GTCATCAAATGGCAAAAGGCCTTTTATAAAGTACTGCAGGAAAAAGCGGGGAAGGATGCCTCGTTTCGCTATG AAATTCGCAAAGTACAAGTAGACGGTAATCATGTTCGGGTCGAAGTAGAAGTGGAAACGAACGGGAAAAAAT GGACCTATGAAATCGAACTGGAGGTCCGTAATGGTAAAATCAAACGTATTCGCCTGCAAGTGGATCCGGAATA TAAAGAAATCGTGCAACTGGCATGGAATCGTACATAA
NT_3	TCTCGCGAGGAAATCCGCAAAGTCGTCGAAACGTGGGTTCGCTTATTCAACAGCGGCGACCCGCGCGACCGC AAAAAATATGAAAAAGCTCAGAAGGAGCTGCTGTCCCCTGACGTTCGCACCGAAATTGGAAATTATACGATCG AACCCGGAACCCTGGAGCGTTTTGTGCAGGCATACTGGAAAGTACTTGATGAGCTTTGGCCGAACGTCCCTAT CCGCGTAGAGATCCGCAAAGTGCAAGTGGATGGCAACCATGTGCGTATTGAGGTCGAAGTAGAAATCAACGG TAAAAAATATACGTTTGAAATTGAAGTCGAGGTGCGTAATGGAAAGATCAAGCGTATTCGTATTCAGCGCGAT CCCGAAATGAAGGAGCTGATCCAGATCGCGTGGAACCGTACCTGA
NT_4	AGTCGTGAAGAAATCCGCAAGGTTGTTGAAACGTACGTTCGCATCTCACTGAGCTCTAGCGAAGAAACCAAAA AAATTCTGCGTGACTTGCTGTCGCCTGACGCACGCTTAGAATTTGGTAACTATACGATCGAATCCGGTGATATT TGGAAATTCATGCAGTTGTTTTGGAAATACTACGCCGGCGACGCACCGCTCCGCCTGGAAATCCGTAAAGTGC AGGTTGATGGTAATCATGTTCGTATCGAAGTCGAAGTCGAGACCAAGGGAAAAAAATGGACCTATGAAATTG AAGTGGAAGTCCGCAACGGTAAAATTAAACGTGTTCGCACCCAAGTTGATCCGGAATATAAGAAAGCATTGCA ATATGCCTGGAACGCAACCTAA
NT_5	TCTCGTGAAGAGATTCGCAAAATCGTGGAGCTCTTTGTAAAAGCATGGGATAATCCTGACGCTCGCGAAAAGT TTGAAAAGAATAAAGACAAGGTATTATCTCCCGATGTCCGTCTGGAAATTGGGAATTTTACCCTGGAAAATAA AGATAAACTTGAATCTTTCTACCGTGTCCTGATCAAACTTTGGCAGGAGAAAGCTGGTCCCAACGTCCGTATCG AGATCCGCAAGGTGCAAGTCGATGGTAACCATGTGCGTGTCGAAGTTGAAGTGGAAACGAATGGCAAAAAAT GGACCTACGAAATTGAAGTAGAAGTTCGTAACGGTACGATTAAACGCATCCGCACTCAGTATGACCCTGAATA TAAAAAGGACATCCAGCAGGCTTGGAACCTCTCATAA

NT_6	AGCCGGGAAGAAATCCGCAAAATTGTGGAAACGATCGTACGTGCGAATCGCGACACGAGTCTCTTTGAGAAG TTAGCCAAAGAACTGAATCTCTTTAGTCCGGACACCCGTATTGAAATTGGCAATTATACTTTTGAAGGGGATGC GATCAAAGTTATCAAAGCGTACATTGAAGCTAATCTGCAGTTCGCGAAAAAGGTTTCGAAAGACGCGCCGGTG CGTATTGAAATCCGTAAAGTGCAAGTGGATGGTAACCACGTTCGTGTTGAGGTTGAAATCGAACTGGCTGGAA AGAAATTTACAACAGAGATCGAGGTTGAAGTGCGCAACGGGGTGGTTAAGCGCATTCGTATTCAAGTCGACC CCGAGTTCAAAAAACTGGTTCAGTACGCTTGGAATAAAACGTAA
NT_7	AGCCGCGAGGAAATTCGGAAGGTGGTAGAAATTTTCATTCGTCTTCAAAGCCTGGACCCGAGCCAGTTAGAAA AAGCTTTAAAAGATTTGAACATTCTTTCGCCGGATGTGCGCCTGGAAGTCGGGAATATCACGCTGAACTCCGC GGATAAACTCATTCGTTTCTTAGCGCTCATTACGGAGATCCTGATTCGCCTGTGGACGGGCAAACCCGCGCCTC TGCGTGTAGAAATCCGTAAAGTGCAGGTAGATGGTAATCACGTGCGCGTGGAGATTGAACAAGAAATTAACG GGCGTAAGTGGACGTACGAAATTGAATTTGAAGTACGCAATGGCGTTATTAAACGTATTCGTGTGCAGCTGGA CCCATCCACCAAAGAGGCTGTCCAGCGTGCATGGAACCTTACCTAA
NT_8	AGTCGCGAGGAAATTCGTAAAGTTGTGGAGACCTTCGTCCGTGCAAAGCAGGATCCGCGTGAATTCACCAAA GCGTTGTCCCTGCTCAGCCCTGATGTTCGGATGGAAATCGGCAACTACACTCTGACCTCCATCCGGGACATTAA ACGCTTTTTCGAGGCCTTAGTAGAAATTTGGAAACGTAAAAACTTGACTGACTGGCGTTACGAAATTCGCAAG GTGCAGGTCGATGGCAATCACGTCCGCATTGAGGTGGAAACACAGACCGACGGCAAAAAATGGACTTGGGAA ATTGAAATCGAAGTACGCAATGGGAAGATCAAACGTATCCGCGAGCAATATGACCCTGAATACAAAAAGGAT GTACAGCTGGCATGGAACCTGACTTGA
NT_9	AGCCGCGAAGAGATCCGCAAAGTTGTCGAGGAGTATATCCGTCTGCTGTATACAGACCCTGATCAGTTCAAGA AAGCGGCCCGCGATAAATTGCTGAGTCCGGATGTGCGTATTGAAATCGGTAATTATACGTTTGATTCCCGCAA CCTCGATCGCTTTCTGGACGCAATGCAGGAATGGGCGAGCCGTTACGATCGTGTGGAAATTCGCAAGGTTCAG GTTGACGGGAACCATGTGCGTGTTGAGATTGAGTTGGAATCGAACGGTAAAAAATGGACGTTTGAAATCGAG GTTGAGGTTCGCAATGGCAAAATTAAGCGCATCCGTCAACAGGTGGATCCGGAATATAAAAAAGTTGTGCAG AATCTGTGGAATAACACGTGA
NT_10	TCCCGGGAAGAGATTCGGAAGGTCGTGGAGACTTGGATCCGCCTTTTTTATAGCTCGGATCCGAACGACTGGG AAACGTTCCAGAAAGCGAAGAAAGATCTGCTCTCACCAGATGTGCGCGTAGAAATCGGAAATTACACGCTTAA TAGTGAACAAGTCGATCGTTGGTGGGAAGCCTGGGTGAAAATCATCCAGAAAGAATTGGAAGAGAAAAACG AACCGCTCCGCACGGAAATTCGCAAGGTTCAAGTGGACGGCAATCACGTACGCGTGGAAATCGAGCAGGAAA AAAACGGCAAGAAGTGGACCTTTGAAGTTGAAGTGGAAGTTCGTAATGGAAAAATCAAGCGTATTCGTCAAC AGGTAGACCCAGAGTACAAAAAGGAGGTCCAGGCGGCTTGGAACAACACCTAA

References

1. Dawson, N.L., Lewis, T.E., Das, S., Lees, J.G., Lee, D., Ashford, P., Orengo, C.A. & Sillitoe, I. CATH: an expanded resource to predict protein function through structure and sequence. *Nucleic Acids Res* **45**, D289-D295 (2017).
2. Kabsch, W. & Sander, C. Dictionary of protein secondary structure: pattern recognition of hydrogen-bonded and geometrical features. *Biopolymers* **22**, 2577-637 (1983).
3. Leaver-Fay, A., Tyka, M., Lewis, S.M., Lange, O.F., Thompson, J., Jacak, R., Kaufman, K., Renfrew, P.D., Smith, C.A., Sheffler, W., Davis, I.W., Cooper, S., Treuille, A., Mandell, D.J., Richter, F., Ban, Y.E., Fleishman, S.J., Corn, J.E., Kim, D.E., Lyskov, S., Berrondo, M., Mentzer, S., Popovic, Z., Havranek, J.J., Karanicolas, J., Das, R., Meiler,

J., Kortemme, T., Gray, J.J., Kuhlman, B., Baker, D. & Bradley, P. ROSETTA3: an object-oriented software suite for the simulation and design of macromolecules. *Methods Enzymol* **487**, 545-74 (2011).
4. Gront, D., Kulp, D.W., Vernon, R.M., Strauss, C.E. & Baker, D. Generalized fragment picking in Rosetta: design, protocols and applications. *PLoS One* **6**, e23294 (2011).
5. Chaudhury, S., Lyskov, S. & Gray, J.J. PyRosetta: a script-based interface for implementing molecular modeling algorithms using Rosetta. *Bioinformatics* **26**, 689-91 (2010).
6. Koga, N., Tatsumi-Koga, R., Liu, G., Xiao, R., Acton, T.B., Montelione, G.T. & Baker, D. Principles for designing ideal protein structures. *Nature* **491**, 222-7 (2012).
7. Shapovalov, M.V. & Dunbrack, R.L., Jr. A smoothed backbone-dependent rotamer library for proteins derived from adaptive kernel density estimates and regressions. *Structure* **19**, 844-58 (2011).
8. Sheffler, W. & Baker, D. RosettaHoles2: a volumetric packing measure for protein structure refinement and validation. *Protein Sci* **19**, 1991-5 (2010).
9. Marcos, E., Basanta, B., Chidyausiku, T.M., Tang, Y., Oberdorfer, G., Liu, G., Swapna, G.V., Guan, R., Silva, D.A., Dou, J., Pereira, J.H., Xiao, R., Sankaran, B., Zwart, P.H., Montelione, G.T. & Baker, D. Principles for designing proteins with cavities formed by curved beta sheets. *Science* **355**, 201-206 (2017).
10. Lawrence, M.C. & Colman, P.M. Shape complementarity at protein/protein interfaces. *J Mol Biol* **234**, 946-50 (1993).
11. Maguire, J.B., Boyken, S.E., Baker, D. & Kuhlman, B. Rapid Sampling of Hydrogen Bond Networks for Computational Protein Design. *J Chem Theory Comput* **14**, 2751-2760 (2018).
12. Smith, C.A. & Kortemme, T. Backrub-like backbone simulation recapitulates natural protein conformational variability and improves mutant side-chain prediction. *J Mol Biol* **380**, 742-56 (2008).
13. Zhang, C., Freddolino, P.L. & Zhang, Y. COFACTOR: improved protein function prediction by combining structure, sequence and protein-protein interaction information. *Nucleic Acids Res* **45**, W291-W299 (2017).
14. Zhou, J. & Grigoryan, G. Rapid search for tertiary fragments reveals protein sequence-structure relationships. *Protein Sci* **24**, 508-24 (2015).
15. Studier, F.W. Protein production by auto-induction in high density shaking cultures. *Protein Expr Purif* **41**, 207-34 (2005).
16. Delaglio, F., Grzesiek, S., Vuister, G.W., Zhu, G., Pfeifer, J. & Bax, A. NMRPipe: a multidimensional spectral processing system based on UNIX pipes. *J Biomol NMR* **6**, 277-93 (1995).
17. Wishart, D.S., Bigam, C.G., Yao, J., Abildgaard, F., Dyson, H.J., Oldfield, E., Markley, J.L. & Sykes, B.D. 1H, 13C and 15N chemical shift referencing in biomolecular NMR. *J Biomol NMR* **6**, 135-40 (1995).
18. Vranken, W.F., Boucher, W., Stevens, T.J., Fogh, R.H., Pajon, A., Llinas, M., Ulrich, E.L., Markley, J.L., Ionides, J. & Laue, E.D. The CCPN data model for NMR spectroscopy: development of a software pipeline. *Proteins* **59**, 687-96 (2005).

19. Cheung, M.S., Maguire, M.L., Stevens, T.J. & Broadhurst, R.W. DANGLE: A Bayesian inferential method for predicting protein backbone dihedral angles and secondary structure. *J Magn Reson* **202**, 223-33 (2010).
20. Rieping, W., Habeck, M., Bardiaux, B., Bernard, A., Malliavin, T.E. & Nilges, M. ARIA2: automated NOE assignment and data integration in NMR structure calculation. *Bioinformatics* **23**, 381-2 (2007).
21. Brunger, A.T., Adams, P.D., Clore, G.M., DeLano, W.L., Gros, P., Grosse-Kunstleve, R.W., Jiang, J.S., Kuszewski, J., Nilges, M., Pannu, N.S., Read, R.J., Rice, L.M., Simonson, T. & Warren, G.L. Crystallography & NMR system: A new software suite for macromolecular structure determination. *Acta Crystallogr D Biol Crystallogr* **54**, 905-21 (1998).
22. Berman, H., Henrick, K. & Nakamura, H. Announcing the worldwide Protein Data Bank. *Nat Struct Biol* **10**, 980 (2003).
23. Bhattacharya, A., Tejero, R. & Montelione, G.T. Evaluating protein structures determined by structural genomics consortia. *Proteins* **66**, 778-95 (2007).
24. Skinner, S.P., Goult, B.T., Fogh, R.H., Boucher, W., Stevens, T.J., Laue, E.D. & Vuister, G.W. Structure calculation, refinement and validation using CcpNmr Analysis. *Acta Crystallogr D Biol Crystallogr* **71**, 154-61 (2015).
25. Winter, G. xia2: an expert system for macromolecular crystallography data reduction. *Journal of Applied Crystallography* **43**, 186-190 (2010).
26. Kabsch, W. Xds. *Acta Crystallogr D Biol Crystallogr* **66**, 125-32 (2010).
27. Evans, P. Scaling and assessment of data quality. *Acta Crystallogr D Biol Crystallogr* **62**, 72-82 (2006).
28. McCoy, A.J., Grosse-Kunstleve, R.W., Adams, P.D., Winn, M.D., Storoni, L.C. & Read, R.J. Phaser crystallographic software. *J Appl Crystallogr* **40**, 658-674 (2007).
29. Adams, P.D., Afonine, P.V., Bunkoczi, G., Chen, V.B., Davis, I.W., Echols, N., Headd, J.J., Hung, L.W., Kapral, G.J., Grosse-Kunstleve, R.W., McCoy, A.J., Moriarty, N.W., Oeffner, R., Read, R.J., Richardson, D.C., Richardson, J.S., Terwilliger, T.C. & Zwart, P.H. PHENIX: a comprehensive Python-based system for macromolecular structure solution. *Acta Crystallogr D Biol Crystallogr* **66**, 213-21 (2010).
30. Kantardjieff, K.A. & Rupp, B. Matthews coefficient probabilities: Improved estimates for unit cell contents of proteins, DNA, and protein-nucleic acid complex crystals. *Protein Sci* **12**, 1865-71 (2003).
31. Weichenberger, C.X. & Rupp, B. Ten years of probabilistic estimates of biocrystal solvent content: new insights via nonparametric kernel density estimate. *Acta Crystallogr D Biol Crystallogr* **70**, 1579-88 (2014).
32. Afonine, P.V., Grosse-Kunstleve, R.W., Echols, N., Headd, J.J., Moriarty, N.W., Mustyakimov, M., Terwilliger, T.C., Urzhumtsev, A., Zwart, P.H. & Adams, P.D. Towards automated crystallographic structure refinement with phenix.refine. *Acta Crystallogr D Biol Crystallogr* **68**, 352-67 (2012).
33. Moriarty, N.W., Grosse-Kunstleve, R.W. & Adams, P.D. electronic Ligand Builder and Optimization Workbench (eLBOW): a tool for ligand coordinate and restraint generation. *Acta Crystallogr D Biol Crystallogr* **65**, 1074-80 (2009).
34. Bernstein, F.C., Koetzle, T.F., Williams, G.J., Meyer, E.F., Jr., Brice, M.D., Rodgers, J.R., Kennard, O., Shimanouchi, T. & Tasumi, M. The Protein Data Bank. A

computer-based archival file for macromolecular structures. *Eur J Biochem* **80**, 319-24 (1977).